VIROLOGY

Inhibition of Polo-like kinase 1 (PLK1) facilitates the elimination of HIV-1 viral reservoirs in CD4$^+$ T cells ex vivo

Dawei Zhou[1], Tsuyoshi Hayashi[2]*, Maxime Jean[2], Weili Kong[1†], Guillaume Fiches[1], Ayan Biswas[1], Shuai Liu[3], Hailemichael O. Yosief[3], Xiaofeng Zhang[3], Jay Bradner[4], Jun Qi[5], Wei Zhang[3], Netty Santoso[1], Jian Zhu[1‡]

Although combination antiretroviral therapy is effective in controlling HIV-1 infection, latent HIV-1 proviruses cannot be eliminated. HIV-1 reactivation induced by the mere use of latency-reversing agents is insufficient to render death of reservoir cells, indicating that certain intrinsic survival mechanisms exist. We report that Polo-like kinase 1 (PLK1) plays a critical role in survival of CD4$^+$ T cells that undergo HIV-1 reactivation from latency or de novo infection. PLK1 is elevated in both scenarios, which requires HIV-1 Nef. HIV-1 enhances PLK1 SUMOylation, causing its nuclear translocation and protein stabilization. Inhibition or knockdown of PLK1 markedly facilitates death of HIV-1–infected CD4$^+$ T cells. Furthermore, PLK1 inhibitors strikingly reduce the size of HIV-1 latent reservoirs in primary CD4$^+$ T cells. Our findings demonstrate that HIV-1 infection hijacks PLK1 to prevent cell death induced by viral cytopathic effects, and that PLK1 is a promising target for chemical "killing" of HIV-1 reservoir cells.

INTRODUCTION

The use of combination antiretroviral therapy (cART) greatly extends the life expectancy of AIDS patients. However, the dormancy of HIV-1 as latent reservoirs, mainly existing in resting CD4$^+$ T cells, confers viral escape from host immune surveillance and/or the effect of cART (*1*–*3*). "Shock and kill" is an actively pursued HIV-1 cure strategy, which relies on the use of latency-reversing agents (LRAs) in the presence of cART to purge HIV-1 latent reservoirs without the induction of global T cell activation, which renders the elimination of CD4$^+$ T cells harboring HIV-1 proviruses either by viral cytopathic effects (CPEs) or by host immunity, especially the cytolytic T lymphocytes (CTLs) (*4*, *5*). However, most of the currently used LRAs, including the histone deacetylase (HDAC) inhibitor vorinostat (also termed SAHA), are unable to reduce HIV-1 latent reservoirs merely by themselves in the clinical setting, despite their potency to induce viral expression of latently infected HIV-1 proviruses (*5*–*7*).

Such current failure indicates that LRAs are able to "shock" but unable to "kill" reservoir cells. HIV-1 uses cellular caspase-dependent or -independent mechanisms to kill host cells in the acute phase, which is mainly exemplified in activated CD4$^+$ T cells (*8*). However, both laboratory and clinical studies indicate that CD4$^+$ T cells and macrophages harboring HIV-1 latent reservoirs have inherent resistance to CTL-mediated cell killing (*9*, *10*). It was also shown that viral CPEs induced by HIV-1 reactivation are not sufficient to lead to the death of reservoir cells (*7*). One possible explanation is that although HIV-1 reactivation induces viral CPEs via one arm, there might be another arm by which HIV-1 reactivation at the same time also turns on certain cell survival mechanisms that hamper virus-induced cell death. For the shock-and-kill cure approach to function, we will probably need to focus more on the kill strategies to facilitate the death of reservoir cells. One idea is to activate HIV-1–specific immune clearance (*7*). However, immune activation is often nonspecific and may lead to autoimmunity. Lately, there have been several reports demonstrating that certain compounds are capable of enhancing the death of HIV-1–reactivated cells or reducing viral reservoirs (*11*–*13*). Although these findings are encouraging, such compounds have received only limited investigation thus far. For example, it is unknown whether these compounds could also facilitate the death of host cells permitting the low-level replication of HIV-1, which represents the neglected "active latency" status and is responsible for replenishing HIV-1 viral reservoirs in lymph nodes even under the pressure of cART (*14*). Therefore, we would like to understand the common cell survival mechanisms associated with both HIV-1 reactivation from latency and HIV-1 de novo infection, which can be targeted to facilitate the elimination of HIV-1 viral reservoirs.

Cell survival or death has long been treated as the physiological outcome of cell cycle control (*15*), in which Polo-like kinase 1 (PLK1) plays a vital role especially for the checkpoint of G_2-to-M transition. Among five known PLKs, PLK1 is the primary one due to its engagement in regulating essentially all of the cell cycle phases, as well as DNA replication, DNA damage response, meiosis, and other "non-canonical" functions (*16*). Beyond cell cycle regulation, PLK1 is also involved in cell survival signaling through the control of pro- and anti-apoptotic machinery. It was shown that some crucial proteins involved in cell survival, including anti-apoptotic Survivin, Stat3, MCL-1, and Bcl-2 (*17*–*19*), or pro-apoptotic Bax, p53, and p73 (*20*–*22*), are positively or negatively regulated by PLK1, respectively. PLK1-mediated cell survival signaling may also be subjected to the upstream regulation of PLK2 in the scenario of mitochondrial dysfunction (*23*). Therefore, in nondividing cells, PLK1 is able to functionally contribute to cell survival through its distinct activity other than cell

[1]Department of Pathology, Ohio State University College of Medicine, Columbus, OH 43210, USA. [2]Department of Microbiology and Immunology, University of Rochester School of Medicine and Dentistry, Rochester NY 14642, USA. [3]Chemistry Department, College of Science and Mathematics, University of Massachusetts at Boston, Boston, MA 02125, USA. [4]Novartis Institutes for BioMedical Research, Cambridge, MA 02139, USA. [5]Dana-Farber Cancer Institute, Department of Medicine, Harvard Medical School, Boston, MA 02115, USA.
*Present address: National Institute of Infectious Diseases, Tokyo 162-8640, Japan.
†Present address: Gladstone Institute of Virology and Immunology, Gladstone Institutes, San Francisco, CA 94158, USA.
‡Corresponding author. Email: jian.zhu@osumc.edu

cycle regulation. Most of the above PLK1 studies have focused on the role of PLK1 in cancer(s). It has been noted that PLK1 expression is elevated in various human cancers, and abnormally elevated expression of PLK1 is often linked to tumor aggressiveness and poor clinical prognosis (*24*). Because both in vitro and in vivo studies showed that the depletion of PLK1 reduces cell survival as well as tumor growth without affecting normal cells, PLK1 inhibitors that disarm its functional kinase domain, reduce its gene expression, or disrupt its interaction with other pivotal cofactors have been actively developed and tested for anticancer therapy (*25*, *26*), while inhibitors targeting PLK1 kinase activity are the most commonly employed ones. In this study, we demonstrate that PLK1 plays a critical role in maintaining the cell survival status of HIV-1–infected $CD4^+$ T cells, a role that has not previously received sustained research attention. We further evaluated the potential of PLK1 kinase inhibitors to facilitate the "killing" of HIV-1–infected $CD4^+$ T cells and the reduction of HIV-1 viral reservoirs in primary resting $CD4^+$ T cells isolated from HIV-1–infected, aviremic subjects ex vivo.

RESULTS

HIV-1 reactivation from latency leads to the elevation of PLK1 protein level

We determined the protein level of PLK1 in CA5 cells, a Jurkat T cell–derived HIV-1 latency cell line harboring replication-competent, green fluorescent protein (GFP)–reporting HIV-1 genome, which were reactivated by tumor necrosis factor–α (TNFα) that induces NF-κB signal. HIV-1 was robustly reactivated in CA5 cells, leading to the elevation of PLK1 protein level that was measured by either immunoblotting (Fig. 1A) or intracellular immunostaining (Fig. 1B). The basal protein and mRNA levels of PLK1 were similar between Jurkat and CA5 cells (fig. S1, A and B). Elevation of PLK1 protein level was observed in CA5 cells treated with TNFα at both low and high doses (fig. S1, C and D). However, there were no such changes in TNFα-treated parental Jurkat cells (Fig. 1, C and D, and fig. S1E). We also tested whether HIV-1 LRAs also have such an effect. Protein kinase C (PKC) agonists (ingenol, prostratin, and bryostatin), HDAC inhibitors (SAHA), and BET inhibitors (JQ1) were used to reactivate latent HIV-1 in CA5 cells (Fig. 1E). Jurkat cells were also treated with these LRAs (Fig. 1F). PKC agonists slightly increased the PLK1 protein level in CA5 cells but markedly decreased it in Jurkat cells. Such effect of ingenol was dose dependent and correlated with ingenol-induced HIV-1 reactivation (fig. S1, F to H). BET inhibitor (BETi) JQ1 moderately increased the PLK1 protein level in CA5 cells while slightly decreasing it in Jurkat cells. HDAC inhibitor SAHA had no effect on PLK1 protein level, likely due to its weak latency-reversing potency in CA5 cells (fig. S1I). The further analysis of PLK1 mRNA level indicated that this LRA treatment causes the reduction of PLK1 transcription to a similar level in both CA5 and Jurkat cells, while TNFα had no such effect (fig. S1, J and K). This indicated that the tested LRAs may have an intrinsic effect leading to the down-regulation of PLK1 gene expression at the transcriptional level and thus likely impair survival of reservoir cells, but LRA-induced HIV-1 reactivation increases the PLK1 protein level that probably counteracts the LRA-mediated PLK1 down-regulation and benefit the survival of HIV-1–reactivated cells. Treatment of J-Lat A2 cells, a Jurkat-derived latency cell line harboring the HIV-1 "LTR-Tat-IRES-GFP" minigenome, and J-Lat 10.6 cells, also a Jurkat-derived latency cell line harboring a near full-length HIV-1 genome deficient in both *env* and *nef* with inserted GFP, failed to cause the elevation of PLK1 protein (fig. S2, A to C). This indicated that some certain viral components missed from the HIV-1 genome mediate such effect, likely *env* and/or *nef*.

We further validated that HIV-1 reactivation induces elevation of PLK1 protein level in a primary $CD4^+$ T cell model, which allows the establishment of HIV-1 latency in the in vitro nonpolarized central memory $CD4^+$ T cells (T_{CM}) by using VSV-G pseudo-typed DHIV viruses with *env* deletion (Fig. 1G) (*27*). HIV-1 reactivation was induced by treating these cells with ingenol, TNFα, and CD3/CD28 antibodies, followed by immunostaining-based measurement of PLK1 and HIV-1 Gag p24 expression (Fig. 1H). TNFα was unable to reactivate latent HIV-1 likely due to the extremely low expression of the TNFα receptor (TNFR) in T_{CM} cells (*28*), resulting in no increase of PLK1. However, treatment of ingenol and CD3/CD28 antibodies caused the elevation of PLK1 protein level, which correlated with their latency-reversing potency (Fig. 1H) (*29*). As a negative control, treatment of the same primary $CD4^+$ T cells without HIV-1 proviruses with ingenol and CD3/CD28 antibodies had no effect on PLK1 protein level (Fig. 1I). Thus, these results support the idea that HIV-1 reactivation from latency increases the PLK1 protein level.

HIV-1 de novo infection in $CD4^+$ T cells leads to the elevation of PLK1 protein level

We next determined whether HIV-1 de novo infection also affects PLK1 protein level. Jurkat cells were infected with wild-type HIV-1 IIIB viruses. PLK1 protein level, but not its mRNA level, increased due to HIV-1 IIIB de novo infection in Jurkat cells (Fig. 2, A and B). The protein level of other PLKs, such as PLK2 and PLK4, was not affected by HIV-1 infection (Fig. 2C), indicating that HIV-1 specifically induces PLK1. Elevation of PLK1 protein level was also confirmed by immunostaining of HIV-1 IIIB–infected Jurkat cells (Fig. 2D). Such change correlated with expression of HIV-1 Gag p24 protein (Fig. 2, A and D). Infection of Jurkat cells with VSV-G pseudo-typed DHIV viruses also led to the elevation of PLK1 protein level, but not its mRNA level (Fig. 2, E and F). To rule out the idea that it is a cell type–specific event, we confirmed the elevation of PLK1 protein level by intracellular immunostaining in HIV-1 IIIB–infected MAGI-HeLa cells, a HeLa-derived cell line stably expressing human CD4 molecule and thus permitting HIV-1 infection (Fig. 2G). We also confirmed that HIV-1 IIIB de novo infection of activated primary $CD4^+$ T cells leads to the elevation of PLK1 protein level (Fig. 2H). Overall, these results show that HIV-1 de novo infection increases PLK1 protein level, similar to the scenario of HIV-1 reactivation from latency.

We next determined which viral protein may mediate the HIV-1–induced elevation of PLK1 protein. As we described, PLK1 protein is not elevated in TNFα-treated J-Lat A2 and 10.6 cells (fig. S2, A to C); however, reactivation of latent VSV-G pseudo-typed DHIV virus (intact *nef,* deleted *env*) (Fig. 1H) or its de novo infection (Fig. 2E) still increases PLK1 protein level, which suggested that HIV-1 Env protein might not be involved. We postulated that the HIV-1 Nef protein is the viral factor that contributes to such effect. It was confirmed by our results showing that stable expression of HIV-1 Nef protein in Jurkat cells led to the increase of PLK1 protein (fig. S2D). Incubation of Jurkat cells with recombinant Nef (rNef) protein also led to the increase of PLK1 protein without causing any obvious cell cytotoxicity (fig. S2, E and F). Next, we used the full-length, replication-competent HIV-1 NL4-3 virus and its *nef*-deficient version (NL4-3 Δ*nef*)

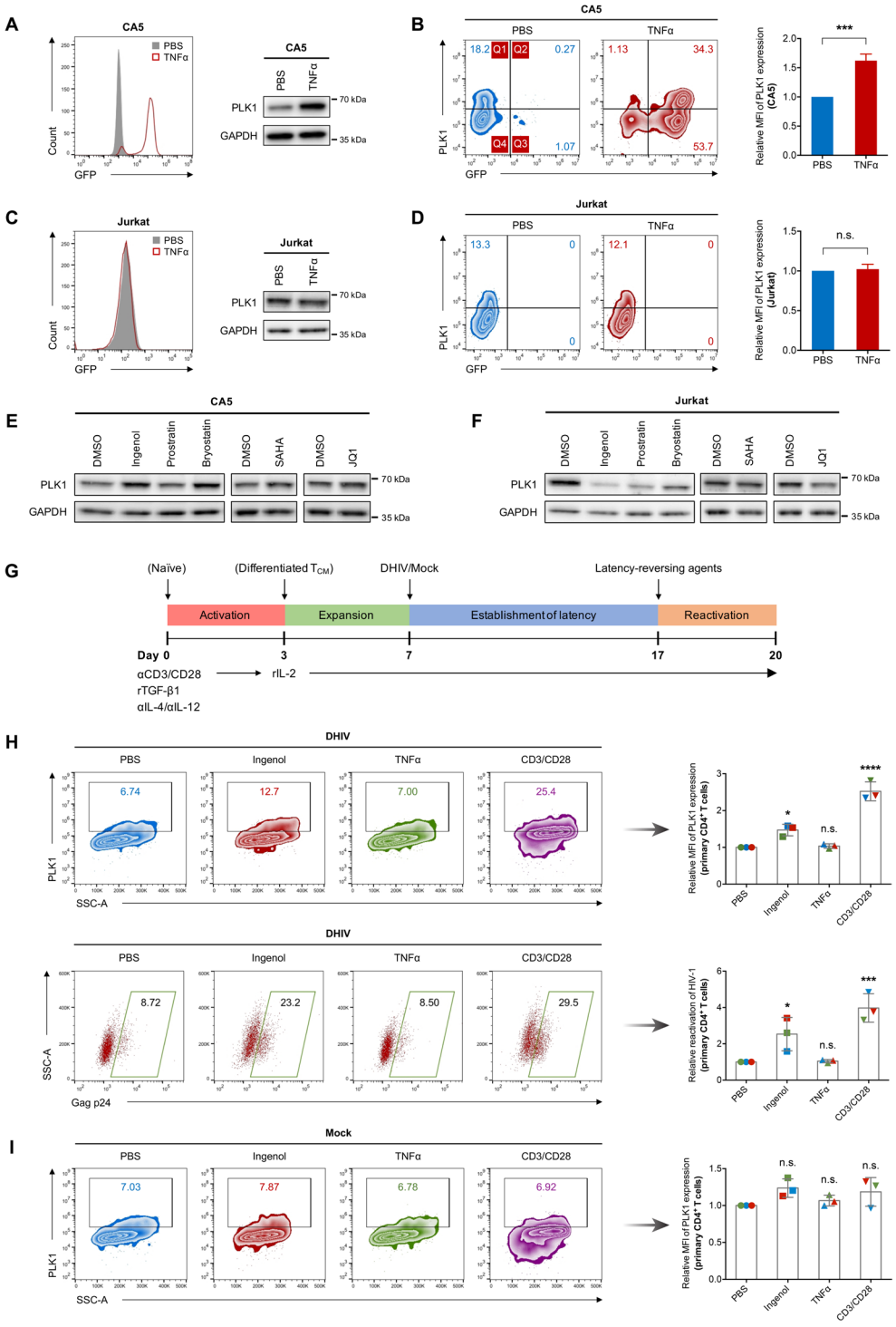

Fig. 1. HIV-1 reactivation from latency increases the protein level of PLK1. (**A** and **C**) HIV-1 reactivation (GFP) and total PLK1 protein in CA5 (A) and Jurkat (C) cells treated with TNFα (10 ng/ml) or PBS [with 1% of bovine serum albumin (BSA)] were measured by flow cytometry and immunoblotting, respectively. (**B** and **D**) Intracellular PLK1 protein level in CA5 (B) and Jurkat (D) cells was measured by immunostaining and flow cytometry. PLK1 was stained by anti-PLK1 primary antibody and subsequent Alexa Fluor 647 (far red)–labeled secondary antibody. For dual-color flow cytometry, cells were gated into four quadrants (B), and (Q1 + Q2) indicates the cell population with the increased PLK1 protein. The mean fluorescence intensity (MFI) was calculated from three independent experiments (***$P \leq 0.001$; n.s., not significant, Student's *t* test). (**E** and **F**) Total protein level of PLK1 in CA5 (E) and Jurkat (F) cells treated with LRAs [ingenol (10 nM), prostratin (500 nM), bryostatin (10 nM), SAHA (1 μM), and JQ1 (1 μM)] or DMSO was measured by immunoblotting. (**G**) HIV-1 latency was established in human T$_{CM}$-like primary CD4$^+$ T cells using DHIV. (**H** and **I**) Intracellular PLK1 protein (top) and reactivated HIV-1 Gag p24 protein (bottom) in HIV-1 latently infected primary CD4$^+$ T cells of one representative donor (H) or noninfected ones of the same donor (I) that were treated with ingenol, TNFα, anti-CD3/CD28 antibodies, or PBS were measured by Zenon dual-color staining (Alexa Fluor 647 for PLK1 and Alexa Fluor 488 for Gag p24) and flow cytometry. Results from three donors were calculated (*$P \leq 0.05$, ***$P \leq 0.001$, ****$P \leq 0.0001$, one-way ANOVA).

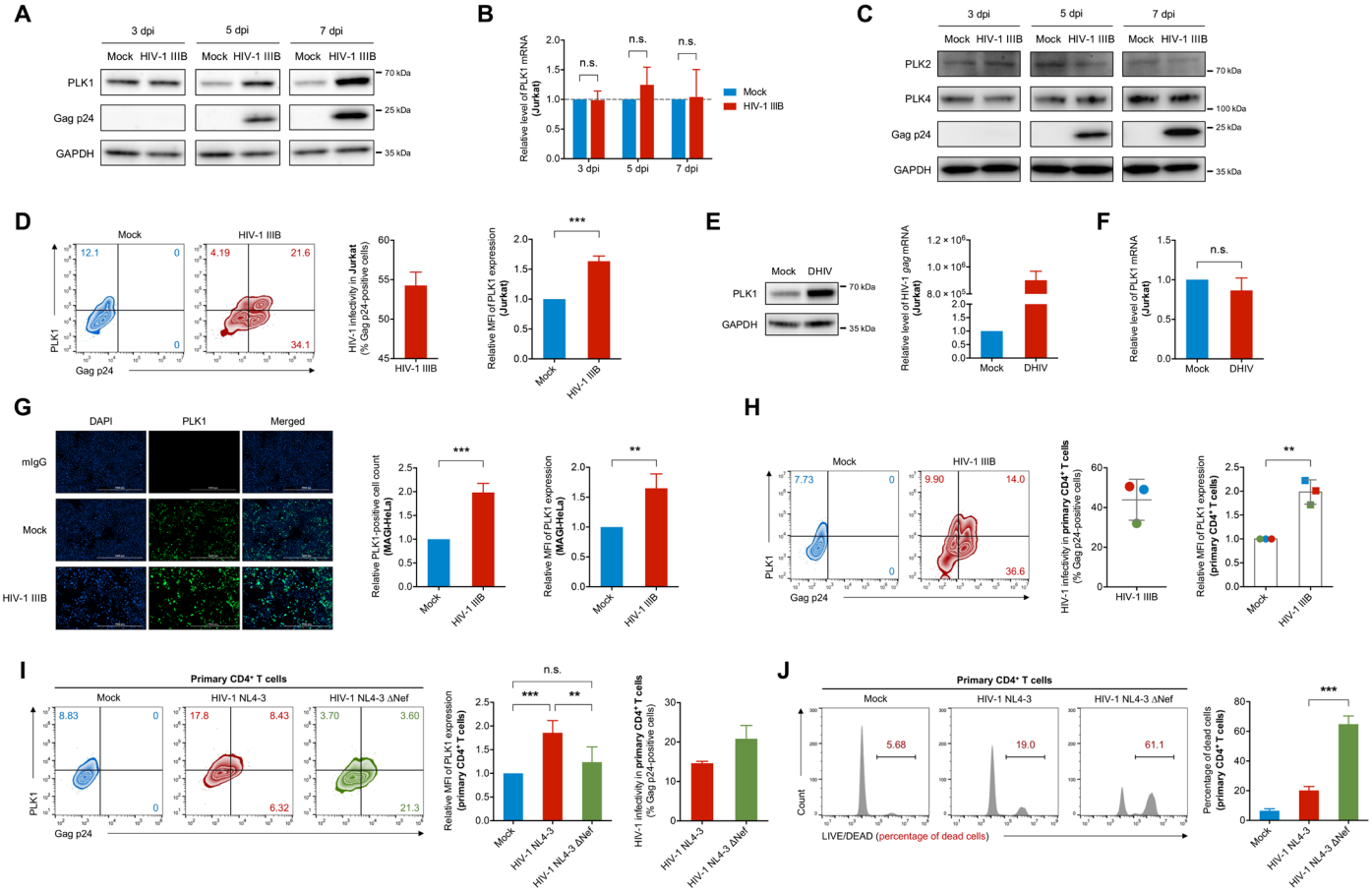

Fig. 2. HIV-1 de novo infection increases the protein level of PLK1. (**A** to **C**) PLK1 (A) and PLK2 and PLK4 (C) in Jurkat cells infected with HIV-1 IIIB (MOI = 1) were measured by immunoblotting. mRNA of PLK1 (B) was measured by RT-qPCR and calculated from three independent experiments (two-way ANOVA). (**D**) PLK1 and HIV-1 Gag p24 in Jurkat cells infected with HIV-1 IIIB or mock at 7 days post infection (dpi) were measured by Zenon dual-color staining. Results were calculated from three independent experiments (***$P \leq 0.001$, Student's *t* test). (**E** and **F**) Protein (E) and mRNA (F) levels of PLK1 in Jurkat cells infected with VSV-G pseudo-typed DHIV (20 ng/ml) were measured by immunoblotting and RT-qPCR, respectively, at 3 dpi. HIV-1 *gag* mRNA was measured by RT-qPCR. RT-qPCR data were calculated from three independent experiments (Student's *t* test). (**G**) PLK1 protein in MAGI-HeLa cells infected with HIV-1 IIIB (MOI = 1) at 3 dpi was measured by immunofluorescence (Alexa Fluor 488). Results were calculated from three independent experiments (**$P \leq 0.01$, ***$P \leq 0.001$, Student's *t* test). (**H**) PLK1 and HIV-1 Gag p24 in $CD4^+$ T cells infected with HIV-1 IIIB (MOI = 1) or mock at 7 dpi were measured by Zenon dual-color staining. Results were calculated from three donors (**$P \leq 0.01$, Student's *t* test). (**I** and **J**) PLK1 and HIV-1 Gag p24 (I), as well as cell death (J) of $CD4^+$ T cells infected with HIV-1 NL4-3, NL4-3 ΔNef (MOI = 1), or mock were measured by Zenon dual-color staining and LIVE/DEAD staining, respectively, at 10 dpi. Results were determined from three replicate experiments (**$P \leq 0.01$, ***$P \leq 0.001$, two-way ANOVA).

to determine the effect of HIV-1 *nef* on PLK1. Consistently, *nef* deficiency abolished the elevation of PLK1 protein induced by infection of HIV-1 NL4-3 virus in Jurkat (fig. S2, G and H) as well as primary $CD4^+$ T cells (Fig. 2I). It is known that HIV Nef protein benefits cell survival (*30*). Aligning with this, we also found that *nef* deficiency promotes more death of HIV-1 NL4-3 virus–infected Jurkat (fig. S2I) as well as primary $CD4^+$ T cells (Fig. 2J). Overall, our results support the idea that HIV-1 Nef is the viral factor that not only contributes to the elevation of PLK1 protein but also enhances cell survival.

HIV-1–induced PLK1 elevation is blocked by inhibition of PI3K and AURKA

It is intriguing to determine which cellular signaling pathway mediates HIV-1–induced PLK1 elevation. It has been reported that PLK1 cross-talks with the phosphoinositide 3-kinase (PI3K) pathway, which mutually affect each other's activity (*31*, *32*), and that the combinatory inhibition of PLK1 and PI3K is an encouraging anticancer therapy (*33*). We first examined whether PI3K is required for HIV-1–induced PLK1 elevation by using three PI3K inhibitors, LY294002, wortmannin, and 3-methyladenine (3-MA). In the scenario of HIV-1 reactivation from latency, CA5 cells were treated with TNFα to induce HIV-1 reactivation, followed by the treatment of PI3K inhibitors or dimethyl sulfoxide (DMSO) control. Measured by intracellular immunostaining, PLK1 protein level was elevated due to TNFα-induced HIV-1 reactivation in CA5 cells, which was significantly impaired by all three PI3K inhibitors (fig. S3A). PI3K inhibitors had no such effect on the basal PLK1 protein level in Jurkat cells treated with TNFα (fig. S3B). In the scenario of HIV-1 de novo infection, Jurkat cells were infected with HIV-1 IIIB viruses, followed by the treatment of PI3K inhibitors or DMSO control. PLK1 protein level was elevated due to HIV-1 de novo infection in Jurkat cells, which was also significantly impaired by all three PI3K inhibitors, while these compounds had no effect on the basal PLK1 protein level (fig. S3C). These data suggest that PI3K kinase activity is required for HIV-1–induced PLK1 elevation. It is worthy to mention that three PI3K inhibitors had a certain moderate but distinct effect on HIV-1

reactivation (fig. S3A) or HIV-1 replication (fig. S3C), but overall, all these compounds consistently block HIV-1–induced PLK1 elevation.

It was reported that PLK1 is regulated by the aurora kinase A (AURKA)–Bora signal, in which Bora acts as a scaffold and molecular chaperone to support the unfolding of PLK1 kinase motif while AURKA is recruited to phosphorylate and activate PLK1 (*34*). In addition, it was shown that HIV-1 infection increases the expression of AURKA (*35*), suggesting that the AURKA-Bora signal could be involved in HIV-1–induced PLK1 elevation. We determined the protein level of AURKA and Bora, as well as the phosphorylation level of AURKA (T288) and PLK1 (T210), the active form of these kinases in cell cycle control, in CA5 or Jurkat cells undergoing HIV-1 reactivation or HIV-1 de novo infection, respectively. The results showed that the protein level of AURKA and PLK1 was increased due to HIV-1 reactivation and HIV-1 de novo infection (fig. S3, D and F), but not in the TNFα-treated and mock-infected Jurkat cells (fig. S3, E and F). However, the protein level of Bora and the phosphorylation level of AURKA and PLK1 were not increased by HIV-1. We next determined whether AURKA kinase is required for HIV-1–induced PLK1 elevation. Similar to PI3K inhibitors (fig. S3, A to C), we treated HIV-1–reactivated CA5 cells and HIV-1 de novo infected Jurkat cells with two AURKA kinase inhibitors, alisertib and tozasertib, followed by the measurement of PLK1 protein level via intracellular immunostaining and flow cytometry. Both AURKA kinase inhibitors impaired the elevation of PLK1 protein induced by HIV-1 reactivation in CA5 cells (fig. S3G), compared to their control groups in Jurkat (fig. S3H). A similar case was seen in the de novo infection of HIV-1 IIIB in Jurkat cells (fig. S3I). We noticed that a certain AURKA kinase inhibitor (alisertib) has the intrinsic effect to induce PLK1 in all treated cells irrelevant to HIV-1 (fig. S3, G to I), likely due to its off-target effect, because such effect of another AURKA kinase inhibitor (tozasertib) was not obvious. Overall, our studies of the cellular signals involved in HIV-1–induced PLK1 elevation suggested that PI3K and AURKA protein kinases are both required.

HIV-1 enhances PLK1 nuclear localization and protein stabilization through its SUMOylation

Our further investigation using confocal microscopy revealed that HIV-1 IIIB infection of MAGI-HeLa cells causes more nuclear distribution of PLK1 protein (Fig. 3A). We also confirmed this in the scenario of HIV-1 reactivation from latency by immunoblotting of PLK1 protein in fractionated nuclear and cytoplasmic extractions of TNFα-treated CA5 cells. It clearly showed that the PLK1 protein level in nuclei, correlating with that in whole cell lysate, is significantly higher in TNFα versus mock-treated [phosphate-buffered saline (PBS)] CA5 cells (Fig. 3B). However, the PLK1 protein level in the cytoplasm is only slightly increased due to TNFα treatment (Fig. 3B). As a negative control, TNFα treatment of Jurkat cells had no such effect, indicating that it is due to HIV-1 reactivation but not TNFα per se (Fig. 3C). There was a recent report showing that protein stability of PLK1 was reinforced through its SUMOylation, followed by its nuclear translocation (*36*). We speculated that HIV-1–induced nuclear accumulation of PLK1 protein is likely due to the increase of its SUMOylation. We immunoprecipitated (IPed) endogenous PLK1 protein from TNFα or mock-treated CA5 cells, and normalized the input for immunoblotting of SUMOylation. TNFα treatment of CA5 cells substantially increased the PLK1 SUMOylation (Fig. 3D), while there was no such effect in TNFα-treated Jurkat cells (Fig. 3E). Meanwhile, it was reported that the proteasome-dependent degradation affects PLK1 protein stability (*37*). We found that MG132 had no effect on PLK1 protein level in TNFα-treated CA5 cells (fig. S4, A and B) but increased it in Jurkat cells (fig. S4C), while MG132 showed a similar increasing effect between CA5 and Jurkat cells in the mock (PBS) condition (fig. S4, B and C), indicating that the proteasome activity is not relevant to HIV-1–induced elevation of PLK1 protein. An earlier report showed that the SUMOylation of PLK1 suppresses its protein ubiquitination and subsequent proteasome-dependent degradation (*36*), which could explain why HIV-1–induced PLK1 SUMOylation enhances its protein stability. We further determined the impact of PLK1 inhibition on its SUMOylation, using a PLK1-specific inhibitor, SBE 13 HCl, which targets PLK1 inactive kinase conformation. There was an obvious reduction of PLK1 SUMOylation in both CA5 and Jurkat cells that were treated with SBE 13 HCl with or without TNFα stimulation, while SBE 13 HCl only caused a slight decrease in total protein level of PLK1 (Fig. 3, F and G). Together, our observation determines that HIV-1 causes the nuclear accumulation of PLK1 protein likely due to the increase of PLK1 SUMOylation, which hinders its proteasome-dependent degradation.

PLK1 inhibition promotes the cell death of HIV-1–infected cells

Given the known functions of PLK1 supporting cell survival (*17*–*23*), we hypothesized that inhibition of PLK1 protein would promote death of HIV-1–infected cells. Treatment of CA5 cells with SBE 13 HCl only led to the weak reactivation of latent HIV-1 even at high concentrations (fig. S5A). For the cell death analysis, we carefully determined the value of 50% cytotoxic concentration (CC_{50}) for SBE 13 HCl in CA5, Jurkat, and primary $CD4^+$ T cells, which are all at a similar range (fig. S5, B to D). We confirmed that compared with control groups (DMSO), treatment of SBE 13 HCl (40 μM) causes more cell death, measured by the LIVE/DEAD assay, in CA5 cells stimulated with ingenol, ingenol + JQ1, or TNFα, respectively (Fig. 4A). However, in Jurkat cells with the same treatments, SBE 13 HCl did not show such an effect (Fig. 4B). At this dose (40 μM), SBE 13 HCl alone showed no obvious cytotoxicity in CA5 and Jurkat cells, nor did it have an effect on reactivation of latent HIV-1 in CA5 cells (fig. S5, E and F). Among these LRAs, ingenol + JQ1 alone showed a considerable cytotoxicity to CA5 cells, likely due to the efficient HIV-1 reactivation. Alternatively, we also measured the viability of the above cells by adenosine 5′-triphosphate (ATP)–based assays. Consistently, the combination of LRAs, especially ingenol and ingenol + JQ1, with SBE 13 HCl markedly reduced cell viability in CA5 cells (fig. S6A) but not in Jurkat cells (fig. S6B).

We also tested SBE 13 HCl in the scenario of HIV-1 de novo infection. Jurkat cells were infected with wild-type HIV-1 NL4-3 or IIIB viruses, followed by the treatment of SBE 13 HCl. The LIVE/DEAD assay showed that SBE 13 HCl causes more drastic cell death of HIV-1–infected cells in a dose-dependent manner, compared to DMSO (Fig. 4C). SBE 13 HCl alone elicited negligible cytotoxicity in these cells at the dose used (60 μM). At the higher dose (80 μM), SBE 13 HCl was able to induce the death of almost all cells, although it alone only caused moderate cytotoxicity in uninfected Jurkat cells. SBE 13 HCl was further tested in the activated naïve primary $CD4^+$ T cells that were challenged with HIV-1 IIIB viruses. Consistently, SBE 13 HCl exhibited a dose-dependent effect to promote the death of HIV-1–infected primary cells (Fig. 4D). Consistent data in HIV-1–infected Jurkat (fig. S6C) and primary $CD4^+$ T cells (fig. S6E) were also observed using the

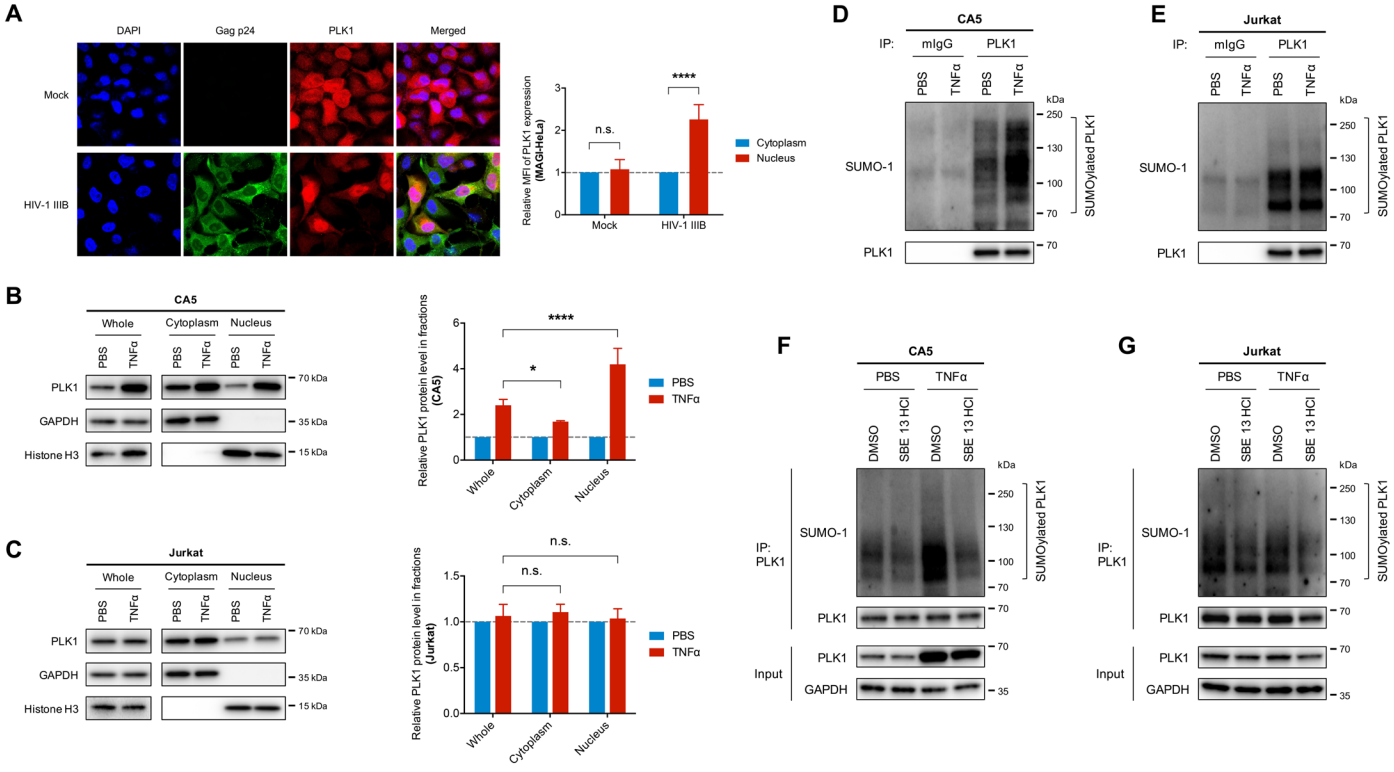

Fig. 3. HIV-1 increases the protein stability and nuclear accumulation of PLK1 through its SUMOylation. (**A**) Intracellular PLK1 and HIV-1 Gag p24 in MAGI-HeLa cells de novo infected with HIV-1 IIIB (MOI = 1) or mock at 3 dpi were measured by Zenon dual-color staining and confocal microscopy. MFI of PLK1 protein in the cytoplasm versus nucleus was determined by analyzing eight fields from four independent experiments (****$P \leq 0.0001$, two-way ANOVA). (**B** and **C**) PLK1 protein level in whole cell lysates or the nuclear and cytoplasmic extractions of TNFα-treated CA5 (B) or Jurkat (C) cells were measured by immunoblotting. The intensity of PLK1 protein was quantified and normalized to the loading controls (GAPDH for whole cell lysates and cytoplasmic fractions, histone H3 for nuclear fraction). Results were calculated from three independent experiments (*$P \leq 0.05$, ****$P \leq 0.0001$, two-way ANOVA). (**D** and **E**) The SUMOylated PLK1 protein in CA5 (D) or Jurkat (E) cells treated with TNFα or PBS was measured by immunoprecipitation (IP) and immunoblotting. Endogenous PLK1 was IPed using its monoclonal antibody. Loading of protein samples was adjusted to assure a similar amount of IPed PLK1 for immunoblotting of SUMOylation. (**F** and **G**) CA5 (F) and Jurkat (G) cells were stimulated with TNFα, followed by the treatment of the PLK1-specific inhibitor SBE 13 HCl (40 μM) for 48 hours. Endogenous PLK1 was IPed and subjected to the detection of its SUMOylation. Loading of samples was adjusted to assure a similar amount of IPed PLK1.

ATP-based assay. We also noticed that SBE 13 HCl treatment decreases, in a dose-dependent manner, the percentage of HIV-1 Gag p24-positive cells in Jurkat (fig. S6D) and primary $CD4^+$ T cells (fig. S6F) undergoing HIV-1 de novo infection. Such an effect is unlikely due to the use of PLK1 inhibitor per se, but rather due to the killing of HIV-1–infected cells, because the fluorescent signals are significantly lost in the dead cells (*38*). It seems that the use of SBE 13 HCl at the higher dose (80 μM) led to the death of cells more than HIV-1–infected ones (~55% of infectivity, estimated from earlier results, Fig. 2D). We postulate that SBE 13 HCl might result in the cell death of a certain uninfected cell population. However, this is not due to the secretion of cytotoxic factors from SBE 13 HCl–treated, HIV-1–infected Jurkat cells (fig. S7). We gauged that other HIV-1–induced, uncharacterized bystander killing effects might play a role, which requires future investigation.

To supplement the results of PLK1 pharmacological inhibition, we also performed a loss-of-function analysis to confirm the role of PLK1 in supporting survival of HIV-1–infected cells. We cloned two sequence-unique PLK1 short hairpin RNAs (shRNAs), along with a nontargeting control shRNA, into the pINDUCER10 lentiviral vector, whose expression can be induced by doxycycline (Dox). CA5 or Jurkat cells stably expressing the above shRNAs were stimulated with ingenol for HIV-1 reactivation, followed by the treatment of Dox to induce shRNA expression leading to the efficient knockdown of endogenous PLK1 protein (Fig. 4, E and G). However, PLK1 knockdown only led to the significant cell death in the ingenol treated CA5 cells (Fig. 4F) but not Jurkat cells (Fig. 4H). These genetic studies further support the notion that inhibition of PLK1 is useful to promote the cell death of HIV-1–infected cells.

Given that AURKA is elevated by HIV-1 infections and that AURKA kinase inhibitors block HIV-1–induced PLK1 elevation, we also determined whether AURKA kinase inhibitors could have a similar effect on the cell death of HIV-1–infected cells as PLK1 kinase inhibitors. However, both LIVE/DEAD and ATP-based assays showed that treatment of AURKA kinase inhibitors alisertib and tozasertib failed to promote more cell death of HIV-1–reactivated CA5 cells than Jurkat cells (fig. S8). One possible reason is that AURKA kinase inhibitors may affect other cellular signals beyond PLK1. It also supported the idea that PLK1 is a unique kinase target for enhancing the cell death of HIV-1–infected cells.

PLK1 inhibition reduces HIV-1 viral reservoirs in primary $CD4^+$ T cells

We expect that because PLK1 inhibition promotes the cell death of HIV-1–reactivated cells, it would cause the reduction of viral

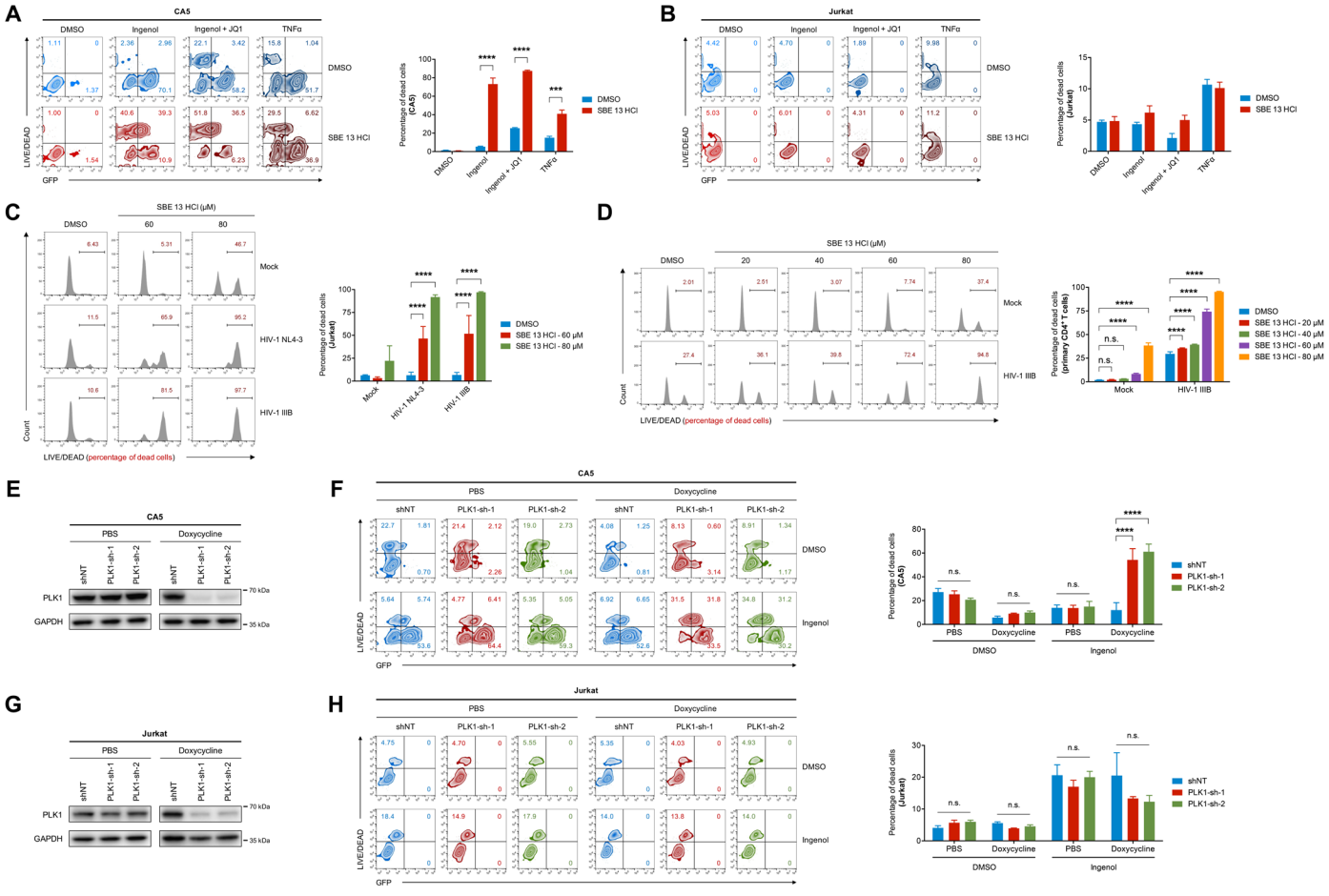

Fig. 4. Inhibition or depletion of PLK1 promotes the cell death of HIV-1–infected CD4$^+$ T cells. (**A** and **B**) Cell death and HIV-1 reactivation in CA5 (A) or Jurkat (B) cells treated with ingenol (10 nM), ingenol (10 nM) + JQ1 (1 μM), or TNFα (10 ng/ml), followed by the further incubation with SBE 13 HCl (40 μM), were measured by the LIVE/DEAD assay. Results were calculated from three independent experiments (***$P \leq 0.001$, ****$P \leq 0.0001$, two-way ANOVA). (**C**) Jurkat cells were de novo infected with HIV-1 NL4-3 or IIIB (MOI = 1) for 7 days, followed by the treatment with SBE 13 HCl (60 and 80 μM). Cell samples were then subjected to the LIVE/DEAD assay. Results were calculated from three independent experiments (****$P \leq 0.0001$, two-way ANOVA). (**D**) Activated primary CD4$^+$ T cells were de novo infected with HIV-1 IIIB (MOI = 1) for 7 days, followed by the treatment with SBE 13 HCl (20, 40, 60, and 80 μM). Cell samples were then subjected to the LIVE/DEAD assay. Results were calculated from three replicates (****$P \leq 0.0001$, two-way ANOVA). (**E** and **G**) CA5 (E) and Jurkat (G) cells stably expressing Dox-inducible PLK1 shRNAs or the nontargeting control one were incubated with Dox. Cellular lysates were then subjected to immunoblotting to confirm the knockdown of PLK1 protein. (**F** and **H**) The above CA5 (E) and Jurkat (G) cells were stimulated with ingenol, followed by the induction of shRNA expression by Dox. Cells were subjected to the LIVE/DEAD assay. Results were calculated from three independent experiments (****$P \leq 0.0001$, two-way ANOVA).

reservoirs in CD4$^+$ T cells that are stimulated with LRAs. To test this, we used the recently reported, TZM-bl–based quantitative viral outgrowth assay (TZA) (*39*) to determine the impact of SBE 13 HCl in combination with LRAs on the size of viral reservoirs in resting CD4$^+$ T cells isolated from HIV-1–positive, aviremic subjects ex vivo. TZA is relatively more timesaving (48 hours of coculture), less expensive (luminescence assay), and less labor-intensive (high-throughput in the 96-well format) compared to the classic quantitative viral outgrowth assay (QVOA). CD4$^+$ T cells isolated from five HIV-1–positive individuals with undetectable viral load were included. From this assay, we noticed that the addition of SBE 13 HCl to ingenol leads to the significant reduction of HIV-1 viral reservoir size in CD4$^+$ T cells, while SBE 13 HCl or ingenol alone had no such effect (Fig. 5A). All of the tested individuals showed the consistent and robust reduction of HIV-1 viral reservoir size in CD4$^+$ T cells (Fig. 5B). These treatments caused negligible cytotoxicity in primary CD4$^+$ T cells (Fig. 5C).

However, TZA has certain issues, such as the disproportionate correlation between the reservoir size and the estimated infectious unit per million (IUPM). Therefore, we also performed the classic QVOA (*40*) to confirm the effect of SBE 13 HCl on the size of HIV-1 viral reservoirs in resting CD4$^+$ T cells ex vivo. By analyzing CD4$^+$ T cells isolated from eight HIV-1–positive individuals with undetectable viral load, treatment of SBE 13 HCl consistently and robustly led to the reduction of reservoir size in resting CD4$^+$ T cells stimulated with ingenol (Fig. 5, D and E), similar to TZA. The results from QVOA and TZA for five overlapped donors showed a decent correlation (Fig. 5F). Overall, from two types of viral outgrowth assays (TZA and QVOA), we observed a similar effect of SBE 13 HCl reducing the size of HIV-1 latent reservoirs ex vivo under the premise of HIV-1 reactivation by using LRAs.

PLK1-BET dual inhibitors reverse HIV-1 latency and decrease viral reservoirs

PLK1-BET dual inhibitors are currently under active development, because PLK1 (kinase) and BRD4 (bromodomain) are the two remarkable targets for anticancer treatment (*41*). Considering the relevance of BRD4 inhibition for shock as well as PLK1 inhibition for kill, we expect that such PLK1-BET dual inhibitors would be useful for the shock-and-kill HIV-1 cure approach. Initially, we screened 24 PLK1-BET dual inhibitors with novel scaffolds (UMB series) (*42*) to identify candidates with potent capability to reactivate latent HIV-1 in J-Lat A2 cells. We identified three candidates, UMB-151, UMB-156, and UMB-158, which have strong latency-reversing potency but weak cytotoxicity (Fig. 6A and fig. S9A). UMB-151, UMB-156, and UMB-158 elicited comparable potency to reactivate latent HIV-1 in both J-Lat A2 (Fig. 6B) and CA5 cells (Fig. 6C) with similar CC_{50} of cytotoxicity (fig. S9, B and C). There are four other candidates—UMB-101, UMB-103, UMB-116, and UMB-152—that are equally potent to reactivate latent HIV-1 but associate with obvious cytotoxicity (fig. S9, A and F). We also demonstrated that the addition of UMB-151 (used as a representative for UMB-151, UMB-156, and UMB-158) to current LRAs, including PKC agonists (prostratin, bryostatin, and ingenol) and HDAC inhibitors (SAHA and entinostat), results in the more efficient reversal of HIV-1 latency (Fig. 6D) without causing more cytotoxicity in CA5 cells (fig. S9, D and E).

We further determined whether PLK1-BET dual inhibitors could have a similar effect on reduction of the HIV-1 latent reservoir size similar to the PLK1-specific inhibitor, SBE 13 HCl. Initially, resting $CD4^+$ T cells isolated from one HIV-1–infected, aviremic individual were treated with JQ1, UMB-151, UMB-156, UMB-158, or UMB-152 in combination with ingenol, or DMSO, followed by TZA to measure the HIV-1 latent reservoir size. Among these tested conditions, only UMB-158 led to the reduction of HIV-1 latent reservoir size (fig. S10). It is worthy to note that although UMB-152 showed much higher cytotoxicity (fig. S9, A and F), it failed to reduce HIV-1 latent reservoir size, indicating that the PLK1-BET dual inhibitor's intrinsic cytotoxicity does not correlate with its effect on reduction of HIV-1 latent reservoir size. We further confirmed such effect of UMB-158 by TZA using $CD4^+$ T cells isolated from three more HIV-1–positive individuals with undetectable viral load (Fig. 6, E and F). UMB-158 alone had no effect on reducing HIV-1 latent reservoir size, likely due to the fact that the PLK1-BET dual inhibitor alone was not efficient to reactivate latent HIV-1, which requires the addition of other types of LRAs. However, we confirmed that the PLK1-BET dual-inhibitor UMB-158 significantly reduces the HIV-1 latent reservoir size under the premise of HIV-1 reactivation in $CD4^+$ T cells once it was combined with ingenol, without causing the obvious cytotoxicity (Fig. 6G). We also confirmed such effect of UMB-158 by classic QVOA using $CD4^+$ T cells isolated from five donors (Fig. 6, H and I). The results from QVOA and TZA for three overlapped

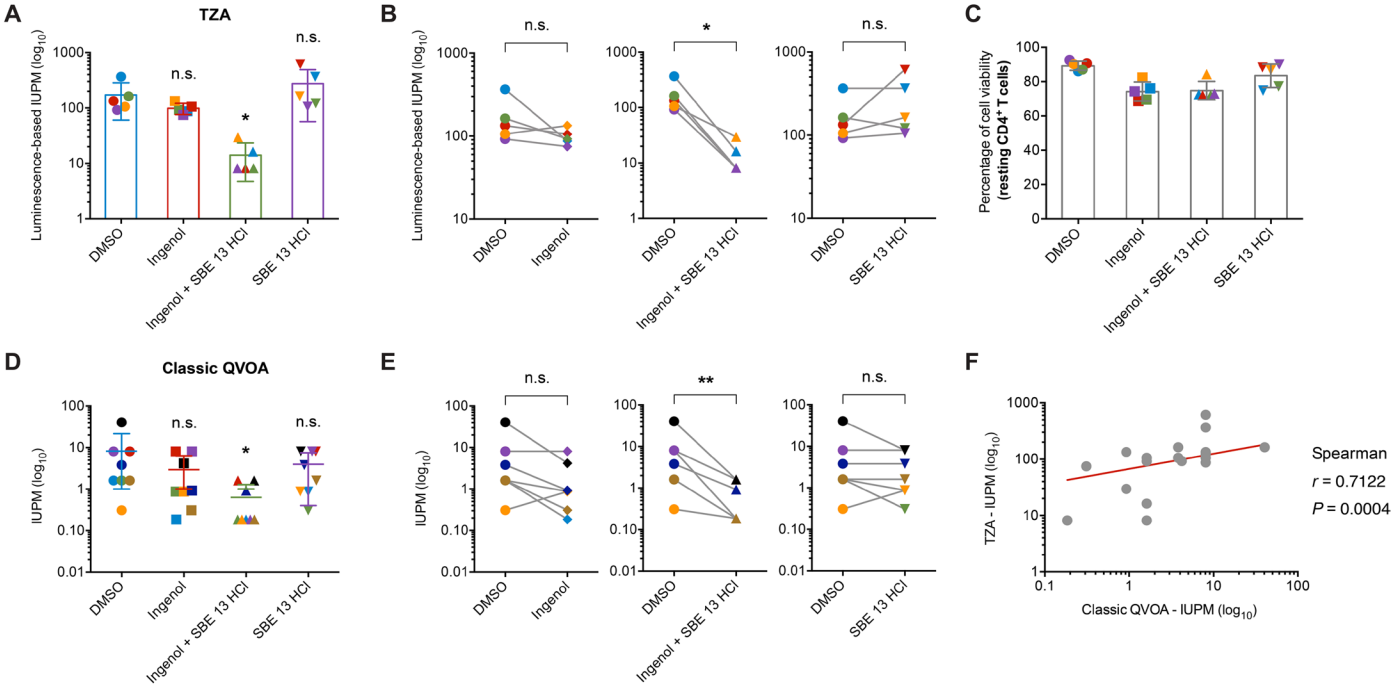

Fig. 5. Inhibition of PLK1 reduces the size of HIV-1 latent reservoirs in $CD4^+$ T cells ex vivo. (**A**) Primary resting $CD4^+$ T cells from five HIV-1–positive, cART-treated, aviremic patients were treated with ingenol (10 nM), SBE 13 HCl (40 μM), or the combination, followed by TZA to measure the size of HIV-1 latent reservoirs. Luminescence-based IUPM was calculated and analyzed by a maximum likelihood estimation method (*$P \leq 0.05$, one-way ANOVA). (**B**) The linked reduction of HIV-1 latent reservoir size across five subjects between two treatments (DMSO versus ingenol, DMSO versus ingenol + SBE 13 HCl, or DMSO versus SBE 13 HCl) from TZA was plotted and analyzed (*$P \leq 0.05$, Student's *t* test). (**C**) The overall cytotoxicity of resting $CD4^+$ T cells caused by the compounds used in (A) and (B) were measured by the LIVE/DEAD assay. (**D**) Resting $CD4^+$ T cells from eight patients were treated with ingenol (10 nM), SBE 13 HCl (40 μM), or the combination, followed by the classic QVOA to measure the size of HIV-1 latent reservoirs. IUPM was estimated by using the same methods as TZA (*$P \leq 0.05$, one-way ANOVA). (**E**) The linked reduction of HIV-1 latent reservoir size across eight subjects between two treatments from QVOA was plotted and analyzed (**$P \leq 0.01$, Student's *t* test). (**F**) Correlation between TZA and QVOA results for the five overlapped subjects was analyzed with the statistical significance (Spearman $r \geq 0.70$, a strong correlation; $P \leq 0.01$, very strong significance).

donors correlated well (Fig. 6J). To conclude, similar to the PLK1-specific inhibitor SBE 13 HCl, the PLK1-BET dual-inhibitor UMB-158 has the potential to efficiently reduce the size of HIV-1 latent reservoirs ex vivo under the premise of HIV-1 reactivation by using LRAs.

DISCUSSION

Although two cases of HIV-1 cure through hematopoietic stem cell transplantation have been reported (*43*, *44*), the shock-and-kill approach remains one of the most investigated HIV-1 cure strategies that can potentially be applied to the general AIDS population. However, the shock-and-kill approach still faces serious barriers, including the failure to eliminate HIV-1 viral reservoirs despite the successful reversal of HIV-1 latency (*7*). On the other hand, the approach to boost immune system, mostly CTLs, for the clearance of HIV-1 reservoir cells is still at the infant stage and needs to be further improved (*7*, *9*). Under this circumstance, several recent studies tried to investigate the cellular mechanisms that contribute to the maintenance of HIV-1 viral reservoirs in host cells. One study demonstrated that retinoic acid-inducible gene-I (RIG-I) determines the status of HIV-1 latent reservoirs, and that acitretin, an FDA (U.S. Food and Drug Administration)–approved retinoic acid (RA) derivative, enhances the RIG-I activity and thus facilitates the killing of reservoir cells through apoptosis (*45*). However, this work was recently challenged by a follow-up study eliciting that such effect of acitretin is inconsistent and poor (*46*). Other studies directly focused on the key regulators of apoptosis, which indicated that HIV-1–infected cells, with either HIV-1 de novo infection or HIV-1 reactivation from latency, can be selectively eliminated by either inhibiting anti-apoptotic factors (Bcl-2, Survivin) or second mitochondria-derived activator of caspases (SMAC) using venetoclax (Bcl-2 inhibitor), YM155 (Survivin inhibitor), or SMAC mimetics, respectively (*11*–*13*). However, it remains unaddressed how these general apoptotic regulators play a distinguished role in regulating cell survival of HIV-1–infected versus uninfected cells.

In our study, we demonstrated that HIV-1 infections, both HIV-1 de novo infection and HIV-1 reactivation from latency, uniquely increase PLK1 protein level through enhancing its SUMOylation in a Nef-associated, PI3K and AURKA-dependent manner, and that PLK1-specific and PLK1-BET dual inhibitors are effective to preferentially promote cell death of HIV-1–infected cells as well as reduce HIV-1 latent reservoirs in $CD4^+$ T cells (Fig. 7). Furthermore, the effect of PLK1 pharmacological inhibition on death of HIV-1–reactivated cells (Fig. 4, A and B, and fig. S6, A and B) was also confirmed by knockdown of PLK1 using its Dox-inducible shRNAs (Fig. 4, E to H). HIV-1 persists at the anatomical sanctuary sites as the latently infected proviruses that undergo spontaneous reactivation or even replicates at the low level (*14*), and we expect that PLK1 inhibition can facilitate the elimination of these two types of reservoir cells, especially with the aid of LRAs to purge latent HIV-1 (Figs. 4 to 6). Our ex vivo, short-term TZA and QVOA evaluation of PLK1 inhibitors (SBE 13 HCl, UMB-158) using primary resting $CD4^+$ T cells isolated from HIV-1–infected, aviremic subjects showed that these compounds by themselves fail to reduce HIV-1 latent reservoirs (Figs. 5, A, B, D, and E, and 6, E, F, H, and I). It is likely due to the fact that SBE 13 HCl alone was unable to reactivate latent HIV-1 (fig. S5, A and E) while the latency-reversing potency of UMB-158 alone was not efficient in $CD4^+$ T cells (Fig. 6, B and C, and fig. S9A). The cytotoxicity of these compounds is quite minimal (Figs. 4, A and B, 5C, and 6G and figs. S5, B to F, S6, A and B, and S9, A to C). On the other hand, LRAs alone failed to reduce HIV-1 latent reservoirs by themselves as well (Figs. 5, A, B, D, and E, and 6, E, F, H, and I, and fig. S10A), although some of them have certain cytotoxicity (Figs. 5C and 6G and fig. S10B). Overall, these results suggest that pharmacological inhibition of PLK1 requires HIV-1 reactivation or active replication that can induce a certain level of CPEs to efficiently promote cell death of reservoir cells and render the reduction of HIV-1 latent reservoir size. Thus, PLK1 inhibitors need to be combined with other LRAs to achieve this goal. In addition, we found that most of the tested LRAs actually reduce PLK1 protein level in Jurkat cells (Fig. 1F), which can be restored by LRA-induced HIV-1 reactivation (Fig. 1E). This could be one reason to explain that although the use of LRAs leads to certain cytotoxicity, HIV-1 reactivation-induced PLK1 elevation may counteract this effect, preventing LRA-mediated killing. We also noticed that the optimized dose of SBE 13 HCl and UMB-158 is different, which may be due to their distinct efficiency of PLK1 inhibition. The UMB series of PLK1-BET dual inhibitors still have a space for improvement by increasing the efficiency of both PLK1 and BET inhibitions, so that such a compound alone can be used for both shock and kill.

Our investigation of viral factors contributing to HIV-1–induced PLK1 elevation identified that HIV-1 Nef is required for such phenomenon (Fig. 2, I and J; fig. S2), which likely increases PLK1 protein through the cellular signaling pathways that involve PI3K and AURKA (fig. S3). AURKA kinase inhibitors were able to block HIV-1–induced PLK1 elevation, but they failed to promote the death of HIV-1–infected cells (fig. S8). One explanation is that pharmacological inhibition of AURKA may generate some adverse effect that compensates for their block of HIV-1–induced PLK1 elevation and prevents cell death, because AURKA is also involved in various other cellular signals (*24*). Moreover, certain AURKA kinase inhibitor (alisertib) up-regulated PLK1 expression (fig. S3, G to I) and the increased PLK1 protein level may actually protect HIV-1–infected cells from death. In addition, these results also suggest that PLK1 is a unique host kinase that can be inhibited for the shock and kill to reduce HIV-1 viral reservoirs, while inhibition of other relevant kinases, such as AURKA, may not necessarily cause the same effect, and that the cytotoxicity caused by these kinase inhibitors does not necessarily correlate with their effect on reduction of HIV-1 viral reservoirs. Our results also showed that HIV-1 infections specifically enhance PLK1 SUMOylation (Fig. 3, D and E), which has been reported to cause PLK1 protein accumulation in nuclei as well as reduction of PLK1 ubiquitination and its proteasome-dependent degradation (*36*). We confirmed these events by our own studies in the scenario of HIV-1 infections (Fig. 3, D and E, and fig. S4). Furthermore, we are the first one to show that the PLK1 inhibitor SBE 13 HCl blocks PLK1 SUMOylation (Fig. 3, F and G). This may explain why PLK1, not other relevant kinases, is uniquely associated with HIV-1 infections. However, we identified that the phosphorylation status of the studied kinases, especially phospho-PLK1-T210, which is essential for its activation in cell cycle progress, is not increased by HIV-1 reactivation from latency or HIV-1 de novo infection, although the protein level of the upstream kinase, AURKA, is up-regulated by HIV-1 (fig. S3, D to F). These data support the idea that the roles of PLK1 in maintenance of cell survival and supervision of cell cycle progress are distinct and subjected to different regulations. We can at least conclude that PLK1 is crucial for maintaining the survival of HIV-1 reservoir $CD4^+$ T cells despite HIV-1 infection–induced CPEs.

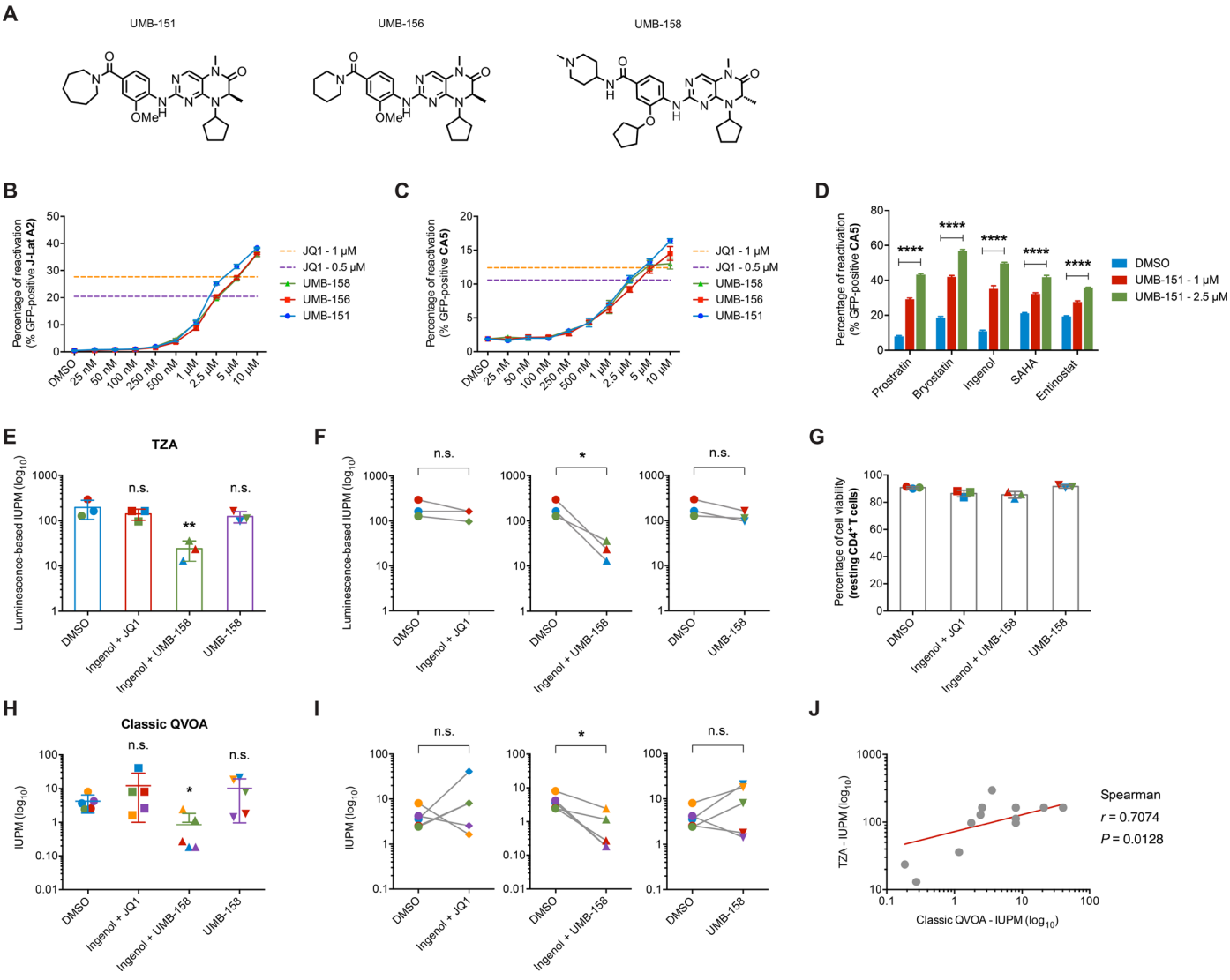

Fig. 6. PLK1-BET dual inhibitors reactivate latent HIV-1 and reduce viral reservoirs in CD4$^+$ T cells. (**A**) Chemical structure of PLK1-BET dual inhibitors (UMB-151, 156, 158). (**B** and **C**) HIV-1 latency-reversing effect of the above PLK1-BET dual inhibitors was titrated in J-Lat A2 (B) and CA5 (C) cells. JQ1 was used as a reference. Results were analyzed from three independent experiments. (**D**) HIV-1 reactivation in CA5 cells treated with UMB-151 and other LRAs [prostratin (100 nM), bryostatin (1 nM), ingenol (1 nM), SAHA (1 μM), and entinostat (10 μM)], alone or in combination, was measured by flow cytometry. Results were compared to DMSO and analyzed from three independent experiments (****$P \leq 0.0001$, two-way ANOVA). (**E** and **F**) Resting CD4$^+$ T cells from three patients were treated with DMSO, ingenol (10 nM) + JQ1 (1 μM), ingenol (10 nM) + UMB-158 (5 μM), or UMB-158 alone (5 μM), followed by TZA. IUPM (E) was calculated (**$P \leq 0.01$, one-way ANOVA). The linked reduction of HIV-1 latent reservoir size across three subjects (F) between two treatments was plotted (*$P \leq 0.05$, Student's *t* test). (**G**) Cytotoxicity of resting CD4$^+$ T cells caused by compounds used in (E) and (F) was measured by LIVE/DEAD assay. (**H** and **I**) Resting CD4$^+$ T cells from five patients were treated with compounds the same as TZA (E), followed by QVOA. IUPM (H) was calculated (*$P \leq 0.05$, one-way ANOVA). The linked reduction of HIV-1 latent reservoir size across five subjects (I) was analyzed (*$P \leq 0.05$, Student's *t* test). (**J**) Correlation between TZA and QVOA results for the three overlapped subjects was analyzed (Spearman $r \geq 0.70$, a strong correlation; $P \leq 0.05$, strong significance).

There are several related issues that remain to be addressed. We noticed that not all HIV-1–infected cells induce PLK1 protein elevation from the immunostaining analysis (Figs. 1B and 2, D and H, and fig. S3, A, C, G, and I). We believe that for the induction of PLK1 protein elevation, HIV-1 Nef protein expressed from HIV-1 proviruses perhaps needs to reach a certain threshold. That could be one reason that not all reactivated or de novo infected HIV-1 can lead to a robust induction of PLK1 protein. In addition, the activation status of cellular signaling, such as PI3K and AURKA, could vary at the single-cell base as well, which would also affect HIV-1–induced PLK1 protein elevation. Technically, the immunofluorescence-based analysis of PLK1 may have a certain detection limit. These speculations will likely be addressed in the future using the single cell–based approaches to investigate the relationship of HIV-1 infection with cellular PLK1 signaling. It is noteworthy that PKC agonists, such as ingenol, cause low level of T cell activation, which may complicate the measurement of the reservoir size. Similar types of LRAs include TLR agonists and NF-κB activators, which are efficient to reverse HIV-1 latency even in vivo (*47*, *48*) but cause low level of T cell activation as well. Some other LRAs, such as HDAC inhibitors (SAHA) and BET inhibitors (JQ1), do not activate CD4$^+$ T cells, but their efficiency to reactivate latent HIV-1 is low to moderate, especially

for primary peripheral $CD4^+$ T cells isolated from AIDS aviremic patients ex vivo (*28*, *49*), which probably would not be ideal LRAs to combine with PLK1 inhibitors. In the future, the combination of our PLK1 inhibitors (SBE 13 HCl and UMB-158) with the panel of all the above LRAs shall be carefully characterized. If identified, other LRAs that can efficiently reactivate latent HIV-1 without causing $CD4^+$ T cell activation shall be used together with PLK1 inhibitors to generate better and safer results. In our studies, the size of HIV-1 latent reservoirs was solely estimated by viral outgrowth assays (TZA and QVOA). Although this approach is standard, it is based on the production of viral particles induced by reactivation and may underestimate the reservoir size. On the contrary, polymerase chain reaction (PCR)–based DNA assays directly quantify HIV-1 proviral DNAs and serve as an important alternative approach, especially those that allow the quantification of intact HIV-1 proviruses (*50*). We did not evaluate PLK1 inhibitors using PCR-based DNA assays, but other studies have shown that the reservoir size estimated by viral outgrowth assays strongly correlates with that measured by PCR-based DNA assays (*39*, *50*, *51*). Nevertheless, it might be a better practice to combine both viral outgrowth and DNA assays for a more comprehensive evaluation in the future. In addition, PLK1 inhibitors were unable to completely eliminate HIV-1 latent reservoirs (Figs. 5, A, B, D, and E, and 6, E, F, H, and I, and fig. S10A), which might be linked to the fact that not all HIV-1–infected cells induce PLK1 protein elevation. This is the limitation of these compounds, suggesting that other killing approaches, such as immunotherapies using the cytotoxic T lymphocytes (CTLs) (*7*), might be needed to combine with PLK1 inhibitors for an ultimate clearance of HIV-1 latent reservoirs, guaranteed for future investigation. Nevertheless, our results undoubtedly showed that PLK1 inhibitors (SBE 13 HCl and UMB-158) significantly reduce the size of HIV-1 latent reservoirs in resting $CD4^+$ T cells isolated from multiple AIDS aviremic patients ex vivo. It is encouraging to launch a more profound analysis, especially in vivo studies including the use of humanized mouse models of HIV-1 infection, for the further evaluation of such potential of PLK1 inhibitors.

Overall, our results recognize that PLK1 is a unique host kinase that is induced by HIV-1 infections and supports the survival of HIV-1–infected cells, and that pharmacological inhibition of PLK1 can be combined with the use of LRAs for the shock-and-kill approach to efficiently eliminate HIV-1 viral reservoirs and ultimately reach a cure of HIV-1. In addition, people currently living with HIV-1 are getting older and are statistically at a higher risk, compared to their HIV-free counterparts, of developing cancer, including AIDS-defining cancers (ADCs), such as Kaposi sarcoma (KS), primary central nervous system lymphoma (PCNSL), cervical carcinoma, and non-Hodgkin lymphoma (NHL) (*52*), as well as non-ADCs (NADCs), such as lung, liver, anal, oral cancers, and Hodgkin lymphoma (*53*). Numerous types of these ADCs and NADCs correlate with abnormal elevated expression of PLK1 (*54*, *55*). Therefore, PLK1 inhibitors can be considered for treating these AIDS-related cancers to reduce the morbidity and mortality, beyond their effect on reducing HIV-1 viral reservoirs.

MATERIALS AND METHODS

Cells culture

Human $CD4^+$ T cell lines, Jurkat, J-Lat A2, J-Lat 10.6, and MOLT-4 $CCR5^+$, were obtained from the National Institutes of Health (NIH) AIDS reagent program. The Jurkat-derived CA5 cell line latently infected with replication-competent, full-length HIV-1 genome was provided by O. Kutsch (University of Alabama). All of the T cell lines were maintained in RPMI 1640 medium (RPMI basic, Sigma-Aldrich) supplemented with 10% fetal bovine serum (FBS) and 1× penicillin-streptomycin solution (Corning). G418 (1 mg/ml; Gibco) was supplemented to culture MOLT-4 $CCR5^+$ cells. Primary cells including patient peripheral blood mononuclear cells (PBMCs), healthy PBMCs, naïve $CD4^+$ T cells, activated $CD4^+$ T cells, and resting $CD4^+$ T cells were maintained in RPMI complete medium (RPMI basic, 1× minimum essential medium nonessential amino acid solution, 1× sodium pyruvate, and 20 mM Hepes). Human recombinant IL-2 (rIL-2, Roche) at 30 U/ml was supplied to primary cells every 2 days. All cryopreserved primary cells were thawed and incubated in RPMI complete medium for 3 days for the thorough recovery before any following treatments. Naïve $CD4^+$ T cells were seeded on a 96-well Nunc-Immuno Maxi Sorp plate (Thermo Fisher Scientific) precoated with soluble anti-CD3/CD28 antibodies (eBioscience, Invitrogen) for 3 days to obtain the activated status. Adherent HEK293T, MAGI-HeLa, TZM-bl cell lines were maintained in Dulbecco's modified Eagle's medium containing 10% FBS and 1× penicillin-streptomycin solution.

Compounds and antibodies

DMSO was obtained from Fisher Scientific. ingenol 3-angelate (also known as PEP005; "ingenol" was used in this study) was purchased from Santa Cruz Biotechnology. Bryostatin-1 ("bryostatin" was used in this study), prostratin, JQ1, and the proteasome inhibitor MG132 were purchased from Sigma-Aldrich. Vorinostat (SAHA), entinostat, LY294002, wortmannin, 3-MA, alisertib, tozasertib, and SBE 13 HCl were purchased from Selleck Chemicals. Recombinant human TNFα was purchased from BD Biosciences. Human TGF-β1 recombinant protein was purchased from R&D Systems. Recombinant HIV-1 Nef protein (rNef) and cART compounds (nevirapine, raltegravir, zidovudine, and efavirenz) were provided by NIH AIDS reagent program. The UMB series of PLK1-BET dual inhibitors were synthesized according to an earlier publication (*42*). The following antibodies were used in this study. Anti-PLK1 was purchased from Sigma-Aldrich. Anti–glyceraldehyde-3-phosphate dehydrogenase (GAPDH), anti-PLK2, anti-PLK4, goat anti-rabbit horseradish peroxidase (HRP)–conjugated secondary antibody, normal mouse IgG, and anti-Bora were purchased from Santa Cruz Biotechnology. Anti-CD3, anti-CD28, Alexa Fluor 488 goat anti-mouse IgG, Alexa Fluor 647 goat anti-mouse IgG, goat anti-mouse HRP-conjugated secondary antibody, anti–HIV-1 Nef, and anti–SUMO-1 antibodies were purchased from Invitrogen. Anti-IL-4 and anti–IL-12 were purchased from R&D Systems. HIV-1 Gag p24 IgG_1 monoclonal antibody was produced from hybridoma cell line (NIH AIDS reagent program). Mouse IgG_{2b} isotype and mouse IgG_1 isotype were purchased from Abcam. Anti-histone H3 was purchased from Active Motif. Biotin-labeled antihuman CD25, antihuman CD69, and antihuman HLA-DR were purchased from Miltenyi Biotec. Anti-AURKA and anti–phospho-AURKA (T288) were purchased from Cell Signaling Technology. Anti–phospho-PLK1 (T210) was purchased from BD Biosciences. For some primary antibodies, they were labeled with isotype-specific fluorophores by using Zenon Alexa Fluor 488 Mouse IgG_1 Labeling Kit or Zenon Alexa Fluor 647 Mouse IgG_{2b} Labeling Kit (Invitrogen) following the manufacturer's instructions. Fluorophore-labeled primary antibodies were mixed for dual-color intracellular staining.

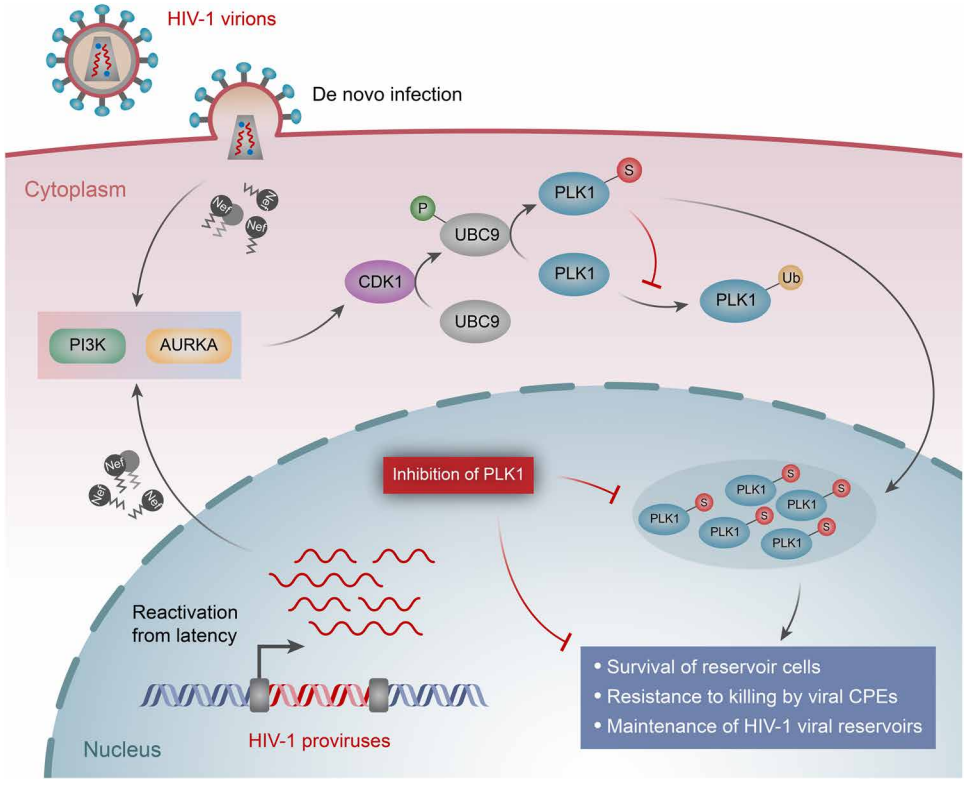

Fig. 7. Inhibition of PLK1 for elimination of HIV-1 viral reservoirs in CD4$^+$ T cells ex vivo. Both HIV-1 de novo infection and reactivation from latency increase the protein level of PLK1, mediated by HIV-1 Nef protein via the signaling pathways involving the PI3K and/or AURKA kinases. HIV-1–induced elevation of PLK1 protein is through enhancing PLK1 SUMOylation that leads to its protein stabilization (by preventing PLK1 ubiquitination) and nuclear accumulation. Activation of CDK1, a downstream kinase of PI3K, was shown to induce phosphorylation of UBC9, a SUMO-conjugating enzyme, causing PLK1 SUMOylation (*36*). Because PLK1 plays a critical role in supporting cell survival, its induction and nuclear accumulation due to HIV-1 infections could counteract the viral CPEs and resist its killing of reservoir cells, thus benefiting the maintenance of HIV-1 viral reservoirs. Therefore, pharmacological inhibition or depletion of PLK1 could synergize with viral CPEs that occur at both conditions of HIV-1 de novo infection and reactivation from latency, and promote the death of HIV-1–reactivated and infected cells and reduce HIV-1 viral reservoirs in CD4$^+$ T cells. Ub, ubiquitination. P, phosphorylation. S, SUMOylation.

HIV-1 infection

HIV-1 NL4-3 wild-type, HIV-1 NL4-3 ΔNef, and HIV-1 IIIB wild-type viruses were provided by NIH AIDS reagent program. HIV-1 NL4-3 wild-type and ΔNef viruses were produced by transfecting HEK293T cells with TurboFect Transfection Reagent (Thermo Fisher Scientific) according to the manuals. Supernatant containing infectious virions was harvested at 48 hours after transfection. HIV-1 IIIB viruses were propagated in activated primary CD4$^+$ T cells. Envelope-deficient DHIV backbone plasmid was provided by Vicente Planelles (*27*). VSV-G pseudo-typed DHIV viruses were prepared by cotransfecting HEK293T cells with DHIV vector and pMD2.G-VSV-G (Addgene) plasmids. Supernatant was harvested at 48 hours after transfection. Supernatant containing viruses was centrifuged to remove cellular debris, filtrated with 0.45-μm membrane filters, and stored at −80°C. Viral stocks were titrated by using quantitative reverse transcription PCR (qRT-PCR) (Clontech) or Gag p24 enzyme-linked immunosorbent assay (Advanced BioScience Laboratories). HIV-1 NL4-3, HIV-1 NL4-3 ΔNef, and IIIB viruses were used for infection at multiplicity of infection (MOI) = 1, and DHIV viruses were used at different concentrations (100 ng/ml for the establishment of primary CD4$^+$ T cell models of HIV-1 latency, and 20 ng/ml for the de novo infection in Jurkat cells). Residual inoculum was washed away at 24 hours after infection. Spinoculation was performed in a 15-ml conical centrifuge tube (Falcon) with 1 ml of antibiotic-free medium containing 1×10^6 cells at 1741*g* at 37°C for 2 hours.

Establishment of HIV-1 latency in human primary CD4$^+$ T cells

A primary CD4$^+$ T cell model of HIV-1 latency was used as previously described with slight modifications (*27*). Human primary CD4$^+$ T cells (Lonza) were stimulated on a 96-well Nunc-Immuno Maxi Sorp plate precoated with soluble anti-CD3/CD28 antibodies in RPMI complete medium containing TGF-β1 (10 ng/ml), antihuman IL-12 (2 μg/ml), and antihuman IL-4 (R&D Systems) (1 μg/ml). At day 3, the naïve cells were considered to be nonpolarized and differentiated into a T_{CM}-like phenotype and were cultured in RPMI complete medium. Human rIL-2 (30 U/ml) was supplemented. At day 7, the T_{CM}-like cells were infected with VSV-G pseudo-typed DHIV (100 ng/ml) through spinoculation, followed by 10-day incubation to allow the establishment of HIV-1 latency. HIV-1 LRAs as well as anti-CD3/CD28 antibodies were used to treat cells for 3 days to reactivate integrated, latently infected HIV-1 proviruses. Cells were then harvested.

Isolation of primary resting CD4$^+$ T cells from human PBMCs

Cryopreserved PBMCs from healthy donors (STEMCELL Technologies) or HIV-1–positive, aviremic individuals with undetectable viral load

were cultured in the RPMI complete medium, supplemented with human rIL-2 (30 U/ml), in the presence of nevirapine (600 nM). Resting $CD4^+$ T cells were isolated by using the $CD4^+$ T cell isolation kit (Miltenyi Biotec), including the negative depletion of cells expressing CD25, CD69, or HLA-DR. Biotin-CD25, CD69, and HLA-DR antibodies (Miltenyi Biotec) were used together with a cocktail of biotin-conjugated antibodies targeting non-$CD4^+$ T cells, which were magnetically depleted by using the $CD4^+$ T Cell MicroBead cocktail following the manufacturer's instructions.

Protein immunoblotting and immunoprecipitation

Cells were harvested, washed twice with 1× D-PBS (Sigma-Aldrich), and pelleted for protein extraction by using 1× radioimmunoprecipitation assay (RIPA) buffer (Upstate, EMD Millipore) containing broad-spectrum protease inhibitors (Thermo Fisher Scientific). Protein concentrations were determined by a BCA protein assay kit (Thermo Fisher Scientific), followed by the electrophoresis on 4 to 20% Tris-Glycine mini gels (Invitrogen). The separated proteins were then transferred to PVDF membranes by an iBlot 2 system (Invitrogen). The membranes were blocked with nonfat milk and incubated overnight with primary antibodies at 4°C with constant rocking. The membranes were washed with 1× PBS-Tween (PBST) and further incubated with secondary antibodies. The membranes were thoroughly washed with 1× PBST and incubated with Clarity Max Western ECL Substrate (Bio-Rad). The immunoblotting images were captured by a FluorChem E imaging system (ProteinSimple). An AlphaView software was used to quantify the intensity of protein bands, which were normalized to the internal loading controls. To determine the PLK1 SUMOylation, endogenous PLK1 was IPed. Pierce Protein A/G Magnetic Beads (Thermo Fisher Scientific) were prewashed with 1× RIPA buffer containing broad-spectrum protease inhibitors. Cellular lysates were precleared with empty magnetic beads for 1 hour at 4°C on a 360° tube rocker. Anti-PLK1 or control IgG antibody was mixed with cellular lysates for incubation overnight at 4°C with constant rotation. New prewashed magnetic beads were added into cellular lysates for another incubation at 4°C for 1 hour with rotation, followed by the centrifugation to collect magnetic beads. Beads containing protein immunocomplexes were washed and subjected to immunoblotting.

Immunofluorescence microscopy

MAGI-HeLa cells were seeded at a density of 4000 cells per well on a 96-well culture plate 1 day before the infection. Cells were infected with HIV-1 IIIB viruses (MOI = 1) for another 3 days. Cells were then fixed with 4% paraformaldehyde at room temperature (RT) for 10 min, followed by permeabilization with 0.2% Triton X-100 at RT for 15 min. The fixed cells were blocked with 1× D-PBS containing 5% FBS for 1 hour at RT and incubated with the primary antibodies in 1× D-PBS containing 2.5% FBS overnight at 4°C. Alexa Fluor 488– or Alexa Fluor 647–conjugated secondary antibodies were then added to cells for another incubation for 1 hour at RT with constant rocking. Nuclei were stained with 4′,6-diamidino-2-phenylindole dye (Invitrogen) for 10 min at RT. Immunostained cells were imaged by using a Cytation 5 multimode reader (BioTek). The mean fluorescence intensity (MFI) and the percentages of GFP-positive cells in each well were quantified by using Gen5 Image$^+$ software (BioTek). For confocal microscopy, MAGI-HeLa cells at 2×10^4 cells per well were seeded on a 24-well culture plate containing circular cover glasses (13 mm) 1 day before the infection. Cells were infected with HIV-1 IIIB, fixed, and permeabilized. The fluorescence-labeled primary antibodies were added to cells for immunostaining. The cover glasses containing cells were mounted onto a microscope slide with ProLong Glass Antifade Mountant (Invitrogen), followed by incubation overnight at 4°C in the dark. Images were acquired using a ZEISS LSM 700 Upright laser scanning confocal microscope with a ZEN imaging software (ZEISS). The MFI of protein expression (cytoplasm versus nucleus) was statistically analyzed by the ImageJ software (NIH).

Flow cytometry

HIV-1 latency cell lines, J-Lat A2, J-Lat 10.6, and CA5 containing integrated, GFP reporter–fused viral genomes, were seeded at 5×10^5 cells/ml and treated with various compounds for 24 to 48 hours. Cells were harvested, washed twice with 1× D-PBS, and analyzed using an Accuri C6 Plus flow cytometer (BD Biosciences) with forward versus side scatter (FSC-A versus SSC-A) gating. For cells that need one-color immunostaining, 1×10^6 cells were washed twice with 1× D-PBS and fixed with 4% paraformaldehyde at RT for 20 min. Pelleted cells were washed and permeabilized with saponin-containing 1× Perm/Wash buffer (BD Biosciences) according to the manufacturer's protocols. Cells were incubated with indicated primary antibodies diluted in 1× Perm/Wash buffer overnight at 4°C, followed by the incubation with fluorophore-conjugated secondary antibodies for 1 hour at RT in the dark. Fluorescence-stained cells were washed three times with 1× Perm/Wash buffer. The staining buffer [1× D-PBS with 2% bovine serum albumin (BSA)] was added to resuspend cells, followed by flow cytometry analysis using the BD Accuri C6 Plus with corresponding optical filters. For cells that need dual-color immunostaining, primary antibodies were labeled separately with Zenon Labeling Kits (Invitrogen), mixed, and incubated with permeabilized cells in 1× Perm/Wash buffer for 30 min at RT. Fluorescence-stained cells were analyzed by flow cytometry. The MFI and the percentage of fluorescence-positive cells were determined by using the FlowJo V10 software.

Nucleus and cytoplasm extraction

CA5 and Jurkat cells were treated with TNFα (10 ng/ml) for 48 hours at a 37°C incubator. Cells (2×10^6) were collected, washed twice with 1× D-PBS, and subjected to nucleus and cytoplasm extraction by using NE-PER Nuclear and Cytoplasmic Extraction Reagents (Thermo Fisher Scientific) following the manufacturer's instructions. Total proteins in the whole cell lysates (W) from the same number of cells were extracted using 1× RIPA buffer. Extracted nuclear (N) and cytoplasmic (C) proteins as well as the whole cell lysate (W) proteins were denatured by 2× SDS sample buffer (Invitrogen) and subjected to immunoblotting analysis with equal loading of extracts. Anti-GAPDH and anti-histone H3 antibodies were used as internal controls to determine the cytoplasmic and nuclear fractions, respectively.

Cell viability assay

The cytotoxicity of compounds was determined by using the ATP-based CellTiter-Glo Luminescent Cell Viability Assay (Promega) and analyzed by the Cytation 5 multimode reader (luminescent mode). CC_{50} was plotted and calculated by using the GraphPad Prism 6.0 software. Death of virus-infected or compound-treated cells was determined by using the LIVE/DEAD Fixable Far Red Dead Cell Stain Kit (Invitrogen) and analyzed by the BD Accuri C6 Plus (flow cytometry).

Quantitative reverse transcription PCR

Quantitative reverse transcription PCR (RT-qPCR) was used to measure the transcriptional levels of studied genes. Briefly, the total RNAs were extracted from cells by using the RNeasy Mini Kit (QIAGEN), followed by the reverse transcription by using the iScript cDNA Synthesis Kit (Bio-Rad). RT-qPCR was performed by using the iTaq Universal SYBR Green Supermix (Bio-Rad) on a CFX Connect Real-Time PCR System (Bio-Rad) as previously described (*56*). The following primers were used in this study: 5′-GAC GCT CTC GCA CCC ATC TC-3′ (HIV-1 *gag*, forward), 5′-CTG AAG CGC GCA CGG CAA-3′ (HIV-1 *gag*, reverse), 5′-TGC TCA AGC CGC ACC AGA-3′ (PLK1, forward), 5′-CCA ACA CCA CGA ACA CGA-3′ (PLK1, reverse), 5′-GCC TCT TGT CTC TTA GAT TTG GTC-3′ (GAPDH, forward), and 5′-TAG CAC TCA CCA TGT AGT TGA GGT-3′ (GAPDH, reverse).

Knockdown of PLK1 using its Dox-inducible shRNAs

The expression of endogenous PLK1 was knocked down in CA5 and Jurkat T cells by its shRNAs expressed from the pINDUCER10 Dox-inducible lentiviral vector, according to the reported protocol (*57*). Briefly, two sequence-unique shRNAs targeting PLK1 (sh-1: 5′-CGA TAC TAC CTA CGG TAA ATT-3′, sh-2: 5′-GTT CTT TAC TTC TGG CTA TAT-3′) and one control shRNA targeting firefly luciferase (shNT: 5′-CAC AAA CGC TCT CAT CGA CAA G-3′) were cloned into the pINDUCER10 vector, which was co-transfected into HEK293T cells with psPAX2 (Addgene) and pMD2.G-VSV-G for production of lentiviruses. CA5 or Jurkat cells were transduced with these lentiviruses, followed by the stable selection and continuous culture in the RPMI medium containing puromycin (1 μg/ml; Gibco). The shRNA stably transduced cells were treated with Dox (5 μg/ml) (Fisher Scientific) for 4 days to induce shRNAs expression.

TZM-bl–based QVOA

The recently reported TZA was used to measure the HIV-1 reservoir size as previously described (*39*). Resting $CD4^+$ T cells isolated from HIV-1–infected, aviremic subjects were treated with LRAs (ingenol or ingenol + JQ1) or PLK1 inhibitors (SBE 13 HCl or UMB-158), alone or in combination, for 48 hours at 37°C. Cells were stimulated with human anti-CD3/CD28 Dynabeads (Gibco) for 4 days in RPMI complete medium containing efavirenz (300 nM). Cells were washed thoroughly with the medium, counted, serially diluted (fourfold), and cocultured with fresh TZM-bl cells seeded on 96-well plates (four replicates for each dilution). Uninfected resting $CD4^+$ T cells from healthy donors were treated similarly in parallel as controls. At 48 hours after co-culturing, TZM-bl cells were harvested for luciferase activity assay (One-Glo System, Promega). Chemiluminescence was determined by using the Cytation 5 multimode reader. Signal from the well containing cells from HIV-1–positive subjects was counted as positive if it exceeded the mean ± 2 SD of the output obtained from the control well (HIV-1–negative subjects). The IUPM representing HIV-1 reservoir size was determined by applying the maximum likelihood estimate via an online tool available at http://silicianolab.johnshopkins.edu/, which was developed by Rosenbloom *et al.* (*58*).

Classic QVOA

The standard QVOA was performed as previously described (*40*) with slight modifications. In brief, resting $CD4^+$ T cells were isolated, serially diluted (fivefold), and incubated with indicated LRAs and/or PLK1 inhibitors for 48 hours, similar to TZA. cART drugs [raltegravir (200 nM), zidovudine (180 nM), and efavirenz (100 nM)] were added throughout the entire viral outgrowth assay to block the re-infection of released viral particles. Compounds were washed away, and cells were stimulated with human anti-CD3/CD28 Dynabeads for 4 days. To carry viral outgrowth, MOLT-4 $CCR5^+$ cells were cocultured with resting $CD4^+$ T cells for 14 days. The supernatant was harvested for detection of released viral particles, by using the ultrasensitive nested RT-qPCR assay as previously described (*56*). The IUPM was estimated by analyzing the data from three replicates for each donor, similar to TZA.

Human subjects

Peripheral whole blood from HIV-1–positive, cART-treated, aviremic patients (viral RNA level ≤ 20 copies/ml; table S1) recruited through the AIDS clinic at the Strong Memorial Hospital of University of Rochester Medical Center (Rochester, NY) was donated via leukapheresis. PBMCs were isolated using the Ficoll-Hypaque gradient method previously described (*56*).

Statistics

The data were statistically analyzed by using the unpaired, two-tailed Student's *t* test or the one-way/two-way analysis of variance (ANOVA). Variables were compared among the outcomes, and the *P* values below 0.05 were considered significant. Correlation analysis was computed by using the Spearman's rank correlation coefficient (*r*) with two-tailed statistical significance (*P*). All of the statistics, presented as means ± SD, were performed by using GraphPad Prism 6.0 software.

Study approval

Written informed consent from the human subjects was received for this study before the enrollment. This study was approved by the University of Rochester Research Subjects Review Board (#RSRB00053667) and The Ohio State University Institutional Review Board (#2018H0161).

SUPPLEMENTARY MATERIALS

Supplementary material for this article is available at http://advances.sciencemag.org/cgi/content/full/6/29/eaba1941/DC1

View/request a protocol for this paper from *Bio-protocol*.

REFERENCES AND NOTES

1. J. K. Wong, M. Hezareh, H. F. Günthard, D. V. Havlir, C. C. Ignacio, C. A. Spina, D. D. Richman, Recovery of replication-competent HIV despite prolonged suppression of plasma viremia. *Science* **278**, 1291–1295 (1997).
2. T. W. Chun, L. Stuyver, S. B. Mizell, L. A. Ehler, J. A. M. Mican, M. Baseler, A. L. Lloyd, M. A. Nowak, A. S. Fauci, Presence of an inducible HIV-1 latent reservoir during highly active antiretroviral therapy. *Proc. Natl. Acad. Sci. U.S.A.* **94**, 13193–13197 (1997).
3. D. Finzi, M. Hermankova, T. Pierson, L. M. Carruth, C. Buck, R. E. Chaisson, T. C. Quinn, K. Chadwick, J. Margolick, R. Brookmeyer, J. Gallant, M. Markowitz, D. D. Ho, D. D. Richman, R. F. Siliciano, Identification of a reservoir for HIV-1 in patients on highly active antiretroviral therapy. *Science* **278**, 1295–1300 (1997).
4. D. S. Ruelas, W. C. Greene, An integrated overview of HIV-1 latency. *Cell* **155**, 519–529 (2013).
5. N. M. Archin, A. L. Liberty, A. D. Kashuba, S. K. Choudhary, J. D. Kuruc, A. M. Crooks, D. C. Parker, E. M. Anderson, M. F. Kearney, M. C. Strain, D. D. Richman, M. G. Hudgens, R. J. Bosch, J. M. Coffin, J. J. Eron, D. J. Hazuda, D. M. Margolis, Administration of vorinostat disrupts HIV-1 latency in patients on antiretroviral therapy. *Nature* **487**, 482–485 (2012).
6. J. D. Siliciano, J. Lai, M. Callender, E. Pitt, H. Zhang, J. B. Margolick, J. E. Gallant, J. Cofrancesco Jr., R. D. Moore, S. J. Gange, R. F. Siliciano, Stability of the latent reservoir for HIV-1 in patients receiving valproic acid. *J Infect Dis* **195**, 833–836 (2007).

7. L. Shan, K. Deng, N. S. Shroff, C. M. Durand, S. A. Rabi, H. C. Yang, H. Zhang, J. B. Margolick, J. N. Blankson, R. F. Siliciano, Stimulation of HIV-1-specific cytolytic T lymphocytes facilitates elimination of latent viral reservoir after virus reactivation. *Immunity* **36**, 491–501 (2012).
8. D. L. Bolton, B. I. Hahn, E. A. Park, L. L. Lehnhoff, F. Hornung, M. J. Lenardo, Death of CD4$^+$ T-cell lines caused by human immunodeficiency virus type 1 does not depend on caspases or apoptosis. *J. Virol.* **76**, 5094–5107 (2002).
9. S.-H. Huang, Y. Ren, A. S. Thomas, D. Chan, S. Mueller, A. R. Ward, S. Patel, C. M. Bollard, C. R. Cruz, S. Karandish, R. Truong, A. B. Macedo, A. Bosque, C. Kovacs, E. Benko, A. Piechocka-Trocha, H. Wong, E. Jeng, D. F. Nixon, Y.-C. Ho, R. F. Siliciano, B. D. Walker, R. B. Jones, Latent HIV reservoirs exhibit inherent resistance to elimination by CD8$^+$ T cells. *J. Clin. Invest.* **128**, 876–889 (2018).
10. K. L. Clayton, D. R. Collins, J. Lengieza, M. Ghebremichael, F. Dotiwala, J. Lieberman, B. D. Walker, Resistance of HIV-infected macrophages to CD8$^+$ T lymphocyte-mediated killing drives activation of the immune system. *Nat. Immunol.* **19**, 475–486 (2018).
11. N. W. Cummins, A. M. Sainski-Nguyen, S. Natesampillai, F. Aboulnasr, S. Kaufmann, A. D. Badley, Maintenance of the HIV reservoir is antagonized by selective BCL2 inhibition. *J. Virol.* **91**, e00012-17 (2017).
12. H.-H. Kuo, R. Ahmad, G. Q. Lee, C. Gao, H.-R. Chen, Z. Ouyang, M. J. Szucs, D. Kim, A. Tsibris, T.-W. Chun, E. Battivelli, E. Verdin, E. S. Rosenberg, S. A. Carr, X. G. Yu, M. Lichterfeld, Anti-apoptotic protein BIRC5 maintains survival of HIV-1-infected CD4$^+$ T cells. *Immunity* **48**, 1183–1194.e5 (2018).
13. G. R. Campbell, R. S. Bruckman, Y.-L. Chu, R. N. Trout, S. A. Spector, SMAC mimetics induce autophagy-dependent apoptosis of HIV-1-infected resting memory CD4+ T cells. *Cell Host Microbe* **24**, **e687**, 689–702 (2018).
14. R. Lorenzo-Redondo, H. R. Fryer, T. Bedford, E.-Y. Kim, J. Archer, S. L. Kosakovsky Pond, Y. S. Chung, S. Penugonda, J. G. Chipman, C. V. Fletcher, T. W. Schacker, M. H. Malim, A. Rambaut, A. T. Haase, A. R. McLean, S. M. Wolinsky, Persistent HIV-1 replication maintains the tissue reservoir during therapy. *Nature* **530**, 51–56 (2016).
15. S. Maddika, S. R. Ande, S. Panigrahi, T. Paranjothy, K. Weglarczyk, A. Zuse, M. Eshraghi, K. D. Manda, E. Wiechec, M. Los, Cell survival, cell death and cell cycle pathways are interconnected: Implications for cancer therapy. *Drug Resist. Updat.* **10**, 13–29 (2007).
16. S. Zitouni, C. Nabais, S. C. Jana, A. Guerrero, M. Bettencourt-Dias, Polo-like kinases: Structural variations lead to multiple functions. *Nat. Rev. Mol. Cell Biol.* **15**, 433–452 (2014).
17. R. Colnaghi, S. P. Wheatley, Liaisons between survivin and Plk1 during cell division and cell death. *J. Biol. Chem.* **285**, 22592–22604 (2010).
18. Y. Zhang, X.-L. Du, C.-J. Wang, D.-C. Lin, X. Ruan, Y.-B. Feng, Y.-Q. Huo, H. Peng, J.-L. Cui, T.-T. Zhang, Y.-Q. Wang, H. Zhang, Q.-M. Zhan, M.-R. Wang, Reciprocal activation between PLK1 and Stat3 contributes to survival and proliferation of esophageal cancer cells. *Gastroenterology* **142**, 521–530.e3 (2012).
19. Y. Ren, C. Bi, X. Zhao, T. Lwin, C. Wang, J. Yuan, A. S. Silva, B. D. Shah, B. Fang, T. Li, J. M. Koomen, H. Jiang, J. C. Chavez, L. V. Pham, P. R. Sudalagunta, L. Wan, X. Wang, W. S. Dalton, L. C. Moscinski, K. H. Shain, J. Vose, J. L. Cleveland, E. M. Sotomayor, K. Fu, J. Tao, PLK1 stabilizes a MYC-dependent kinase network in aggressive B cell lymphomas. *J. Clin. Invest.* **128**, 5517–5530 (2018).
20. X. Liu, R. L. Erikson, Polo-like kinase (Plk)1 depletion induces apoptosis in cancer cells. *Proc. Natl. Acad. Sci. U.S.A.* **100**, 5789–5794 (2003).
21. K. Ando, T. Ozaki, H. Yamamoto, K. Furuya, M. Hosoda, S. Hayashi, M. Fukuzawa, A. Nakagawara, Polo-like kinase 1 (Plk1) inhibits p53 function by physical interaction and phosphorylation. *J. Biol. Chem.* **279**, 25549–25561 (2004).
22. N. Koida, T. Ozaki, H. Yamamoto, S. Ono, T. Koda, K. Ando, R. Okoshi, T. Kamijo, K. Omura, A. Nakagawara, Inhibitory role of Plk1 in the regulation of p73-dependent apoptosis through physical interaction and phosphorylation. *J. Biol. Chem.* **283**, 8555–8563 (2008).
23. T. Matsumoto, P.-Y. Wang, W. Ma, H. J. Sung, S. Matoba, P. M. Hwang, Polo-like kinases mediate cell survival in mitochondrial dysfunction. *Proc. Natl. Acad. Sci. U.S.A.* **106**, 14542–14546 (2009).
24. S. M. A. Lens, E. E. Voest, R. H. Medema, Shared and separate functions of polo-like kinases and aurora kinases in cancer. *Nat. Rev. Cancer* **10**, 825–841 (2010).
25. X. Liu, M. Lei, R. L. Erikson, Normal cells, but not cancer cells, survive severe Plk1 depletion. *Mol. Cell. Biol.* **26**, 2093–2108 (2006).
26. K. Strebhardt, Multifaceted polo-like kinases: Drug targets and antitargets for cancer therapy. *Nat. Rev. Drug Discov.* **9**, 643–660 (2010).
27. A. Bosque, V. Planelles, Induction of HIV-1 latency and reactivation in primary memory CD4$^+$ T cells. *Blood* **113**, 58–65 (2009).
28. C. A. Spina, J. Anderson, N. M. Archin, A. Bosque, J. Chan, M. Famiglietti, W. C. Greene, A. Kashuba, S. R. Lewin, D. M. Margolis, M. Mau, D. Ruelas, S. Saleh, K. Shirakawa, R. F. Siliciano, A. Singhania, P. C. Soto, V. H. Terry, E. Verdin, C. Woelk, S. Wooden, S. Xing, V. Planelles, An in-depth comparison of latent HIV-1 reactivation in multiple cell model systems and resting CD4+ T cells from aviremic patients. *PLOS Pathog.* **9**, e1003834 (2013).
29. G. Jiang, E. A. Mendes, P. Kaiser, D. P. Wong, Y. Tang, I. Cai, A. Fenton, G. P. Melcher, J. E. K. Hildreth, G. R. Thompson, J. K. Wong, S. Dandekar, Synergistic reactivation of latent HIV expression by ingenol-3-angelate, PEP005, targeted NF-kB signaling in combination with JQ1 induced p-TEFb activation. *PLOS Pathog.* **11**, e1005066 (2015).
30. S. D. Briggs, B. Scholtz, J. M. Jacque, S. Swingler, M. Stevenson, T. E. Smithgall, HIV-1 Nef promotes survival of myeloid cells by a Stat3-dependent pathway. *J. Biol. Chem.* **276**, 25605–25611 (2001).
31. K. Kasahara, H. Goto, I. Izawa, T. Kiyono, N. Watanabe, S. Elowe, E. A. Nigg, M. Inagaki, PI 3-kinase-dependent phosphorylation of Plk1-Ser99 promotes association with 14-3-3γ and is required for metaphase-anaphase transition. *Nat. Commun.* **4**, 1882 (2013).
32. Z. Li, J. Li, P. Bi, Y. Lu, G. Burcham, B. D. Elzey, T. Ratliff, S. F. Konieczny, N. Ahmad, S. Kuang, X. Liu, Plk1 phosphorylation of PTEN causes a tumor-promoting metabolic state. *Mol. Cell. Biol.* **34**, 3642–3661 (2014).
33. D. De Martino, E. Yilmaz, A. Orlacchio, M. Ranieri, K. Zhao, A. D. Cristofano, PI3K blockage synergizes with PLK1 inhibition preventing endoreduplication and enhancing apoptosis in anaplastic thyroid cancer. *Cancer Lett.* **439**, 56–65 (2018).
34. A. Seki, J. A. Coppinger, C.-Y. Jang, J. R. Yates, G. Fang, Bora and the kinase Aurora a cooperatively activate the kinase Plk1 and control mitotic entry. *Science* **320**, 1655–1658 (2008).
35. J. D. Lapek Jr., M. K. Lewinski, J. M. Wozniak, J. Guatelli, D. J. Gonzalez, Quantitative temporal viromics of an inducible HIV-1 model yields insight to global host targets and phospho-dynamics associated with protein Vpr. *Mol. Cell. Proteomics* **16**, 1447–1461 (2017).
36. D. Wen, J. Wu, L. Wang, Z. Fu, SUMOylation promotes nuclear import and stabilization of polo-like kinase 1 to support its mitotic function. *Cell Rep.* **21**, 2147–2159 (2017).
37. D. Kang, J. Chen, J. Wong, G. Fang, The checkpoint protein Chfr is a ligase that ubiquitinates Plk1 and inhibits Cdc2 at the G2 to M transition. *J. Cell Biol.* **156**, 249–259 (2002).
38. N. W. Cummins, A. M. Sainski, H. Dai, S. Natesampillai, Y. P. Pang, G. D. Bren, M. C. M. de Araujo Correia, R. Sampath, S. A. Rizza, D. O'Brien, J. D. Yao, S. H. Kaufmann, A. D. Badley, Prime, shock, and kill: Priming CD4 T cells from HIV patients with a BCL-2 antagonist before HIV reactivation reduces HIV reservoir size. *J. Virol.* **90**, 4032–4048 (2016).
39. A. Sanyal, R. B. Mailliard, C. R. Rinaldo, D. Ratner, M. Ding, Y. Chen, J. M. Zerbato, N. S. Giacobbi, N. J. Venkatachari, B. K. Patterson, A. Chargin, N. Sluis-Cremer, P. Gupta, Novel assay reveals a large, inducible, replication-competent HIV-1 reservoir in resting CD4$^+$ T cells. *Nat. Med.* **23**, 885–889 (2017).
40. G. M. Laird, E. E. Eisele, S. A. Rabi, J. Lai, S. Chioma, J. N. Blankson, J. D. Siliciano, R. F. Siliciano, Rapid quantification of the latent reservoir for HIV-1 using a viral outgrowth assay. *PLOS Pathog.* **9**, e1003398 (2013).
41. P. Ciceri, S. Müller, A. O'Mahony, O. Fedorov, P. Filippakopoulos, J. P. Hunt, E. A. Lasater, G. Pallares, S. Picaud, C. Wells, S. Martin, L. M. Wodicka, N. P. Shah, D. K. Treiber, S. Knapp, Dual kinase-bromodomain inhibitors for rationally designed polypharmacology. *Nat. Chem. Biol.* **10**, 305–312 (2014).
42. S. Liu, H. O. Yosief, L. Dai, H. Huang, G. Dhawan, X. Zhang, A. M. Muthengi, J. Roberts, D. L. Buckley, J. A. Perry, L. Wu, J. E. Bradner, J. Qi, W. Zhang, Structure-guided design and development of potent and selective dual bromodomain 4 (BRD4)/polo-like kinase 1 (PLK1) inhibitors. *J. Med. Chem.* **61**, 7785–7795 (2018).
43. G. Hütter, D. Nowak, M. Mossner, S. Ganepola, A. Müssig, K. Allers, T. Schneider, J. Hofmann, C. Kücherer, O. Blau, I. W. Blau, W. K. Hofmann, E. Thiel, Long-term control of HIV by CCR5 Delta32/Delta32 stem-cell transplantation. *N. Engl. J. Med.* **360**, 692–698 (2009).
44. R. K. Gupta, S. Abdul-Jawad, L. E. McCoy, H. P. Mok, D. Peppa, M. Salgado, J. Martinez-Picado, M. Nijhuis, A. M. J. Wensing, H. Lee, P. Grant, E. Nastouli, J. Lambert, M. Pace, F. Salasc, C. Monit, A. J. Innes, L. Muir, L. Waters, J. Frater, A. M. L. Lever, S. G. Edwards, I. H. Gabriel, E. Olavarria, HIV-1 remission following CCR5Δ32/Δ32 haematopoietic stem-cell transplantation. *Nature* **568**, 244–248 (2019).
45. P. Li, P. Kaiser, H. W. Lampiris, P. Kim, S. A. Yukl, D. V. Havlir, W. C. Greene, J. K. Wong, Stimulating the RIG-I pathway to kill cells in the latent HIV reservoir following viral reactivation. *Nat. Med.* **22**, 807–811 (2016).
46. E. Garcia-Vidal, M. Castellví, M. Pujantell, R. Badia, A. Jou, L. Gomez, T. Puig, B. Clotet, E. Ballana, E. Riveira-Muñoz, J. A. Esté, Evaluation of the innate immune modulator acitretin as a strategy to clear the HIV reservoir. *Antimicrob. Agents Chemother.* **61**, e01368-17 (2017).
47. A. B. Macedo, C. L. Novis, C. M. De Assis, E. S. Sorensen, P. Moszczynski, S.-H. Huang, Y. Ren, A. M. Spivak, R. B. Jones, V. Planelles, A. Bosque, Dual TLR2 and TLR7 agonists as HIV latency-reversing agents. *JCI Insight* **3**, e122673 (2018).
48. C. C. Nixon, M. Mavigner, G. C. Sampey, A. D. Brooks, R. A. Spagnuolo, D. M. Irlbeck, C. Mattingly, P. T. Ho, N. Schoof, C. G. Cammon, G. K. Tharp, M. Kanke, Z. Wang, R. A. Cleary, A. A. Upadhyay, C. de, S. R. Wills, S. D. Falcinelli, C. Galardi, H. Walum, N. J. Schramm, J. Deutsch, J. D. Lifson, C. M. Fennessey, B. F. Keele, S. Jean, S. Maguire, B. Liao, E. P. Browne, R. G. Ferris, J. H. Brehm, D. Favre, T. H. Vanderford, S. E. Bosinger, C. D. Jones, J. P. Routy, N. M. Archin, D. M. Margolis, A. Wahl, R. M. Dunham, G. Silvestri, A. Chahroudi, J. V. Garcia, Systemic HIV and SIV latency reversal via non-canonical NF-κB signalling in vivo. *Nature* **578**, 160–165 (2020).

49. N. M. Archin, J. L. Kirchherr, J. A. M. Sung, G. Clutton, K. Sholtis, Y. Xu, B. Allard, E. Stuelke, A. D. Kashuba, J. D. Kuruc, J. Eron, C. L. Gay, N. Goonetilleke, D. M. Margolis, Interval dosing with the HDAC inhibitor vorinostat effectively reverses HIV latency. *J. Clin. Invest.* **127**, 3126–3135 (2017).
50. K. M. Bruner, Z. Wang, F. R. Simonetti, A. M. Bender, K. J. Kwon, S. Sengupta, E. J. Fray, S. A. Beg, A. A. R. Antar, K. M. Jenike, L. N. Bertagnolli, A. A. Capoferri, J. T. Kufera, A. Timmons, C. Nobles, J. Gregg, N. Wada, Y.-C. Ho, H. Zhang, J. B. Margolick, J. N. Blankson, S. G. Deeks, F. D. Bushman, J. D. Siliciano, G. M. Laird, R. F. Siliciano, A quantitative approach for measuring the reservoir of latent HIV-1 proviruses. *Nature* **566**, 120–125 (2019).
51. M. Kiselinova, W. de Spiegelaere, M. J. Buzon, E. Malatinkova, M. Lichterfeld, L. Vandekerckhove, Integrated and total HIV-1 DNA predict ex vivo viral outgrowth. *PLOS Pathog.* **12**, e1005472 (2016).
52. A. E. Grulich, M. T. van Leeuwen, M. O. Falster, C. M. Vajdic, Incidence of cancers in people with HIV/AIDS compared with immunosuppressed transplant recipients: A meta-analysis. *Lancet* **370**, 59–67 (2007).
53. C.-C. Wang, M. J. Silverberg, D. I. Abrams, Non-AIDS-defining malignancies in the HIV-infected population. *Curr. Infect. Dis. Rep.* **16**, 406 (2014).
54. N. Takai, R. Hamanaka, J. Yoshimatsu, I. Miyakawa, Polo-like kinases (Plks) and cancer. *Oncogene* **24**, 287–291 (2005).
55. L. Liu, M. Zhang, P. Zou, Expression of PLK1 and survivin in non-Hodgkin's lymphoma treated with CHOP. *Acta Pharmacol. Sin.* **29**, 371–375 (2008).
56. M. J. Jean, T. Hayashi, H. Huang, J. Brennan, S. Simpson, A. Purmal, K. Gurova, M. C. Keefer, J. J. Kobie, N. G. Santoso, J. Zhu, Curaxin CBL0100 blocks HIV-1 replication and reactivation through inhibition of viral transcriptional elongation. *Front. Microbiol.* **8**, 2007 (2017).
57. K. L. Meerbrey, G. Hu, J. D. Kessler, K. Roarty, M. Z. Li, J. E. Fang, J. I. Herschkowitz, A. E. Burrows, A. Ciccia, T. Sun, E. M. Schmitt, R. J. Bernardi, X. Fu, C. S. Bland, T. A. Cooper, R. Schiff, J. M. Rosen, T. F. Westbrook, S. J. Elledge, The pINDUCER lentiviral toolkit for inducible RNA interference in vitro and in vivo. *Proc. Natl. Acad. Sci. U.S.A.* **108**, 3665–3670 (2011).
58. D. I. Rosenbloom, O. Elliott, A. L. Hill, T. J. Henrich, J. M. Siliciano, R. F. Siliciano, Designing and interpreting limiting dilution assays: General principles and applications to the latent reservoir for human immunodeficiency virus-1. *Open Forum Infect. Dis.* **2**, ofv123 (2015).

Acknowledgments: We thank V. Planelles (University of Utah) for providing the DHIV viral vector and O. Kutsch (University of Alabama at Birmingham) for providing the CA5 cells. We also thank the members of OSU Center for Retrovirus Research (P. Green, S. -L. Liu, L. Wu, N. Liyanage, and A. Sharma), S. Maggirwar (George Washington University), S. Dewhurst (University of Rochester), and J. Kobie (University of Alabama at Birmingham) for helpful comments and feedback. **Funding:** This study was funded by NIH research grants R01AI150448, R01DE025447, and R33AI116180 to J.Z. and R03DE029716 to N.S. and research grant U54CA156732 to J.B. and W.Z. **Author contributions:** J.Z. and D.Z. conceived and designed this study; D.Z. performed most of the experiments; T.H. and M.J. provided experimental support; D.Z., N.S., and J.Z. analyzed the results; T.H., M.J., W.K., G.F., A.B., S.L., H.O.Y., X.Z., J.B., J.Q., and W.Z. contributed reagents and/or provided advice regarding this study; D.Z. and J.Z. wrote the manuscript; A.B. reviewed the manuscript; and J.Z. supervised the entire study. **Competing interests:** J.Q. has consulting roles for K-group Alpha, K-group Beta, and Epiphanes. The remaining authors declare that they have no competing interests. **Data and materials availability:** All data needed to evaluate the conclusions in the paper are present in the paper and/or the Supplementary Materials. Additional data and materials related to this paper may be requested from the authors.

Submitted 14 December 2019
Accepted 14 May 2020
Published 15 July 2020
10.1126/sciadv.aba1941

Citation: D. Zhou, T. Hayashi, M. Jean, W. Kong, G. Fiches, A. Biswas, S. Liu, H. O. Yosief, X. Zhang, J. Bradner, J. Qi, W. Zhang, N. Santoso, J. Zhu, Inhibition of Polo-like kinase 1 (PLK1) facilitates the elimination of HIV-1 viral reservoirs in $CD4^+$ T cells ex vivo. *Sci. Adv.* **6**, eaba1941 (2020).

ScienceAdvances

Inhibition of Polo-like kinase 1 (PLK1) facilitates the elimination of HIV-1 viral reservoirs in CD4 $^{+}$ T cells ex vivo

Dawei Zhou, Tsuyoshi Hayashi, Maxime Jean, Weili Kong, Guillaume Fiches, Ayan Biswas, Shuai Liu, Hailemichael O. Yosief, Xiaofeng Zhang, Jay Bradner, Jun Qi, Wei Zhang, Netty Santoso and Jian Zhu

Sci Adv **6** (29), eaba1941.
DOI: 10.1126/sciadv.aba1941